9/01/2025

EL 6743 & EL 6744, AEA 051-001 Central Australia Minerals Project Joint Partial Surrender Report

06-May-2022 to 07-Nov-2025

Contents

Summary of all activities conducted 4

Key words **4**

1. Introduction 7

1.1 Location and Access **7**

1.2 Tenure History **7**

1.3 Exploration Rationale and Targets **8**

2. Geology 8

2.1 Basinal Framework **8**

Eromanga Basin (Early Jurassic - Late Cretaceous) 8

Musgraves Basement **9**

2.3 Relevant minerals systems **10**

Sandstone-hosted Uranium 10

Orthomagmatic Ni-Cu ± PGE in ultramafic complexes 14

2.4 Prior Exploration: Historic and Recent Work **15**

Uranium (Eromanga Basin) 15

Diamonds (Musgrave Basement) 17

Base and precious metals (Ni-Cu-PGE) 19

3. Exploration over the life of the tenure 22

3.1 Geophysics – airborne surveys **22**

Geophysical processing and integration 22

3.2 Target generation, evaluation and rationale for surrender **26**

Conclusion 27

References 28

Company Reports **30**

Appendix 1 31

Report Type	Partial Surrender Report
Reporting Period	06-May-2022 to 05-May-2024
Tenement number(s)	EL 6743 & EL 6744
Project Name	AEA 051-001 Central Australia Minerals Project (SA)
EL Holder	Tri-Star Minerals Pty Ltd (100%)
Authors	Michael Tschaban, Jesse Savage & Rafaella Gallagher (Minerals), Trish O'Sullivan (Acting Tenure Manager).
Date of Report	09-January-2025
Contact details	Tri-Star Minerals Pty Ltd PO Box 7128, BRISBANE QLD 4000
Telephone	(07) 3236 9800
Facsimile	(07) 3221 2146
Email for technical data	tenures@tri-stargroup.com
Email for expenditure	tenures@tri-stargroup.com

Summary of all activities conducted

EL 6743 is part of the AEA051-001 Central Australia Minerals Project, comprising four contiguous Exploration Licences of 3,591 km^2, located over the Eastern Musgraves Province – Pedirka/ Warburton Basins on the South Australia - Northern Territory border.

EL 6743 comprises an area of 913 km^2, of which 360 km^2 (39 %) was surrendered. EL 6744 comprises an area of 995 km^2, of which 324 km^2 (32 %) was surrendered.

This Partial Surrender Report outlines all the work completed from the date of grant (06 May 2022) to 05 November 2024.

Work over the surrendered portion of the ELs consisted of desktop data compilation and target generation work prior to May 2024, followed by a regional Falcon Airborne Gravity Gradiometery (AGG) survey of 20,729 line kilometres (over a large portion of SA). 465 line km of this was flown over the original extents of EL 6743 and 480 line km over EL 6744 at 1 km north-south line spacing, not including turn-arounds or tie-lines. Note the total given for the project area (1,844 line km) does include the lines outside and around the border of the ELs.

After the data was received, it was processed and integrated with existing geophysical datasets, and a comprehensive review of targets and company strategy followed. (Survey data - see SARIG Website)

Table 1. Summary of work over EL 6743 & EL 6744

Year	Activity	Comment
1 (to 05/23)	Desktop studies	Data compilation
2 (to 05/24)	1,844 line km AGG (25.5%)	Falcon Airborne Gravity Gradiometry
3 (to 05/25)	Desktop studies	Geophysical integration, prospectivity modelling

Key words

Abminga, Amadeus Basin, Birksgate Complex, Broken Hill Type, Bulldog Shale, Central Australia Minerals Project, Eromanga Basin, Fregon Domain, Giles Magmatic Event, Kulgera Granites, Musgrave Mobile Belt, Orthomagmatic, Pedirka Basin, Pitjantjatjara Supersuite, Tri-Star, Warburton Basin.

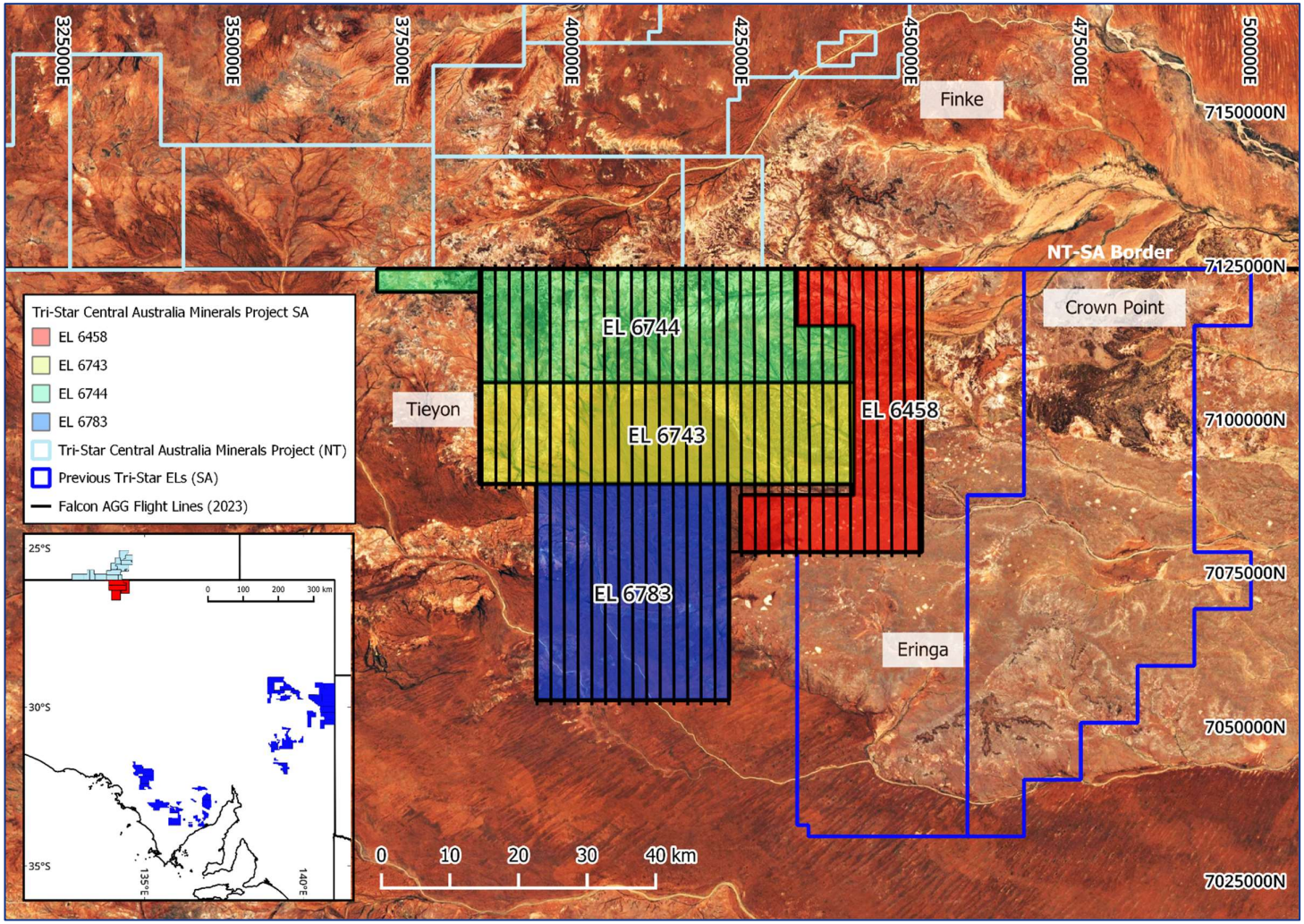

Figure 1. AEA051-001 Central Australia Minerals Project Exploration Index Map (GDA 2020) showing tenure and location of work over EL 6743 & EL 6744

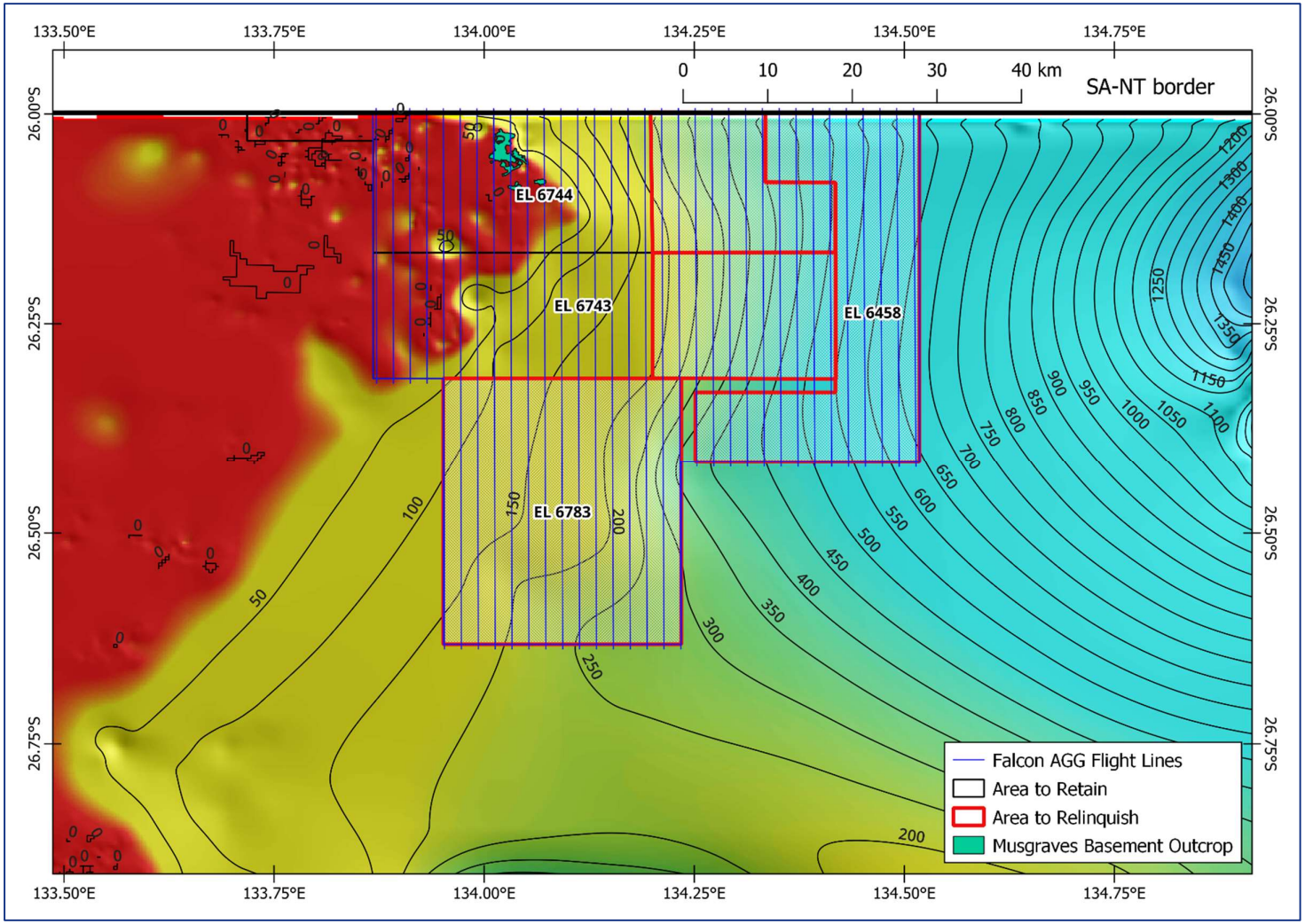

Figure 2. Area relinquished from EL 6743 & EL 6744 shown over basement depth contours and colour stretch

1. Introduction

This Introduction provides information on the EL's Location (1.1), Tenure History (1.2) and Tri-Star's current exploration strategy within the Central Australia Minerals Project (1.3).

Section 2 outlines the geology of the overlying basins relevant to the project area (2.1), a review of what is known of the Eastern Musgraves and its tectonic boundaries (2.2), and the mineral systems that the company is targeting (2.3). Previous work within the project area is discussed in Section 2.4.

Section 3 describes the Falcon Airborne Gravity Gradiometry (AGG) survey undertaken in Year 2 (2023 field season), as well as subsequent processing, targeting and the rationale for surrender.

1.1 Location and Access

EL 6743 & EL 6744 are two of four fully contiguous Exploration Licences (ELs) of 3,591 km^2 along the norther border of South Australia. The ELs currently comprises an area of 913 and 995 km^{2,}, and were reduced to 553 km^2 and 671 km^2 through relinquishment of 360 km^2 and 324 km^2 (Figure 2).

The project is 280 km south of Alice Springs (NT), which is the nearest population centre, and 190 km north of Oonadatta (SA). The surrendered portion of EL 6744 spans the 5645 Tieyon and 5745 Treloar 1:100,000 map sheets and is encompassed within the SG5310 Abminga 1:250,000 sheet.

Road access to the area is via the A87 Sturt Highway south from Alice Springs, or north from Coober Pedy, then via unsealed roads and station tracks to project areas.

Elevation decreases directly east-northeast throughout the tenement package. The Fregon Domain of the Proterozoic Musgrave Basement outcrops in the west of the EL package, and is overlain by units of the Cambrian-Devonian Warburton Basin and the Early Jurassic to Late Cretaceous Eromanga Basin to the east (Figure 12). The digital elevation model produced from laser scanner data on the Falcon AGG system, coupled with the Geoscience Australia DEM-S (ANGG19) data is shown in Figure 12.

The EL is encompassed within the Native Title Determinations of the Walka Wani Aboriginal Corporation.

1.2 Tenure History

EL 6743 & EL 6744 were granted to Tri-Star Minerals Pty Ltd on the 6th May 2022 for a period of six years, as an area of 913 km^2 and 995 km^2 respectively.

This report outlines all activities undertaken over the surrendered portions of EL 6743 & EL 6744 within Year 1 and 2 of the tenure.

Licence	Grant Date	Current Year	Original Area	Surrendered Area
EL 6743	06/05/2022	3	913 km^2	360 km^2
EL 6744	06/05/2022	3	995 km^2	324 km^2

1.3 Exploration Rationale and Targets

Tri-Star is primarily targeting Uranium resources conducive to in situ leaching in South Australia.

However, given the prospectivity of the basement in the Central Australia region, metalliferous commodities are also targeted as part of the Eastern Musgraves exploration strategy that extends into the Northern Territory. This strategy prioritises orthomagmatic nickel-copper, potential BHT deposits and epigenetic Cu-Au.

2. Geology

EL 6743 & EL 6744 overlie an area in which the basement of the Eastern Musgrave Province's Fregon Domain is overlain by sediments of the Late Triassic-Cretaceous Eromanga Basin, which is in turn overlain by the < 5 Ma Stevenson Paleochannel and Hamilton Paleovalley.

2.1 Basinal Framework

Eromanga Basin (Early Jurassic - Late Cretaceous)

The Eromanga Basin is laterally extensive across eastern Australia, and these units make up the majority of the geology at surface over the eastern project area. The older Jurassic sequences are mainly terrestrial (fluvial quartzite) with interbedded carbonaceous shale, while the Cretaceous sequences of the inland seaway are transgressive and later, regressive marine facies (Munson 2013).

The Cretaceous sequences of the basin host the largest collection of sandstone-hosted uranium resources in Australia south of the project area, in the Frome Embayment (Callabonna Sub-basin), discussed further in Section 2.3.

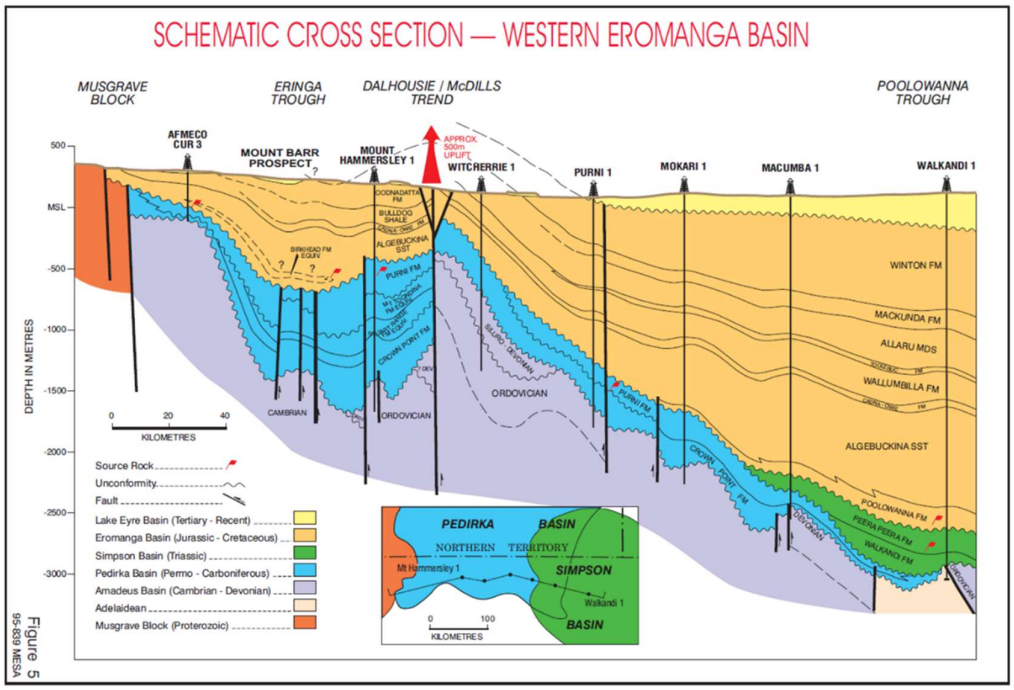

Figure 3. Cross section of the Eromanga Basin in South Australia overlying units of the Pedirka Basin (from Alexander & Jensen-Schmidt 1995)

Musgraves Basement

The Musgraves basement disappears to depth beneath basins that deepen eastward, where its relationship to the North Australia Craton and potentially the Thompson Orogen is unknown (Purdy et al 2013).

The Musgrave Province is a mobile belt between cratons, comprised of Mesoproterozoic to early Cambrian sequences (Wade et al 2008), deformed through multiple episodes that essentially record supercontinental cycles, intruded by voluminous magmatism, and exhumed from beneath the Central Australia Superbasin by the Petermann and Alice Springs Orogenies (Aitken & Betts 2009a).

The oldest sequences of the province are the Musgravian Gneiss (such as the Birksgate Complex of the project area), emplaced in an arc setting recycling juvenile crust from 1600-1540 Ma. The felsic crust is metamorphosed to amphibolite, and even granulite facies, and later intruded by mafics and ultramafics of the 1090–1040 Ma Giles Suite (Close 2013).

Of relevance to potential minerals systems is the 1090–1040 Ma Giles Magmatic Event, in which the 1075 Ma Warakurna Large Igneous Province was emplaced within the Western-Central Musgraves (Smithies et al 2008, 2013). The thickest centre of magmatism directly underlies the West Musgraves, where it hosts orthomagmatic nickel sulphide deposits (including Nebo-Babel). Combined seismic-gravity modelling imaged a thick magmatic underplate beneath the entire province (>45 km), and the variations in thickness show magmatic centres following craton margins (or lithospheric ‘steps’) at the time of emplacement (Alghamdi et al 2017).

The Musgraves province is prospective for not only orthomagmatic nickel-copper and PGE systems associated with the LIP, but orogenic and intrusion-related gold, IOCGs and even Broken Hill Type (BHT) deposits (Woodhouse & Gum 2003, Joly et al 2014).

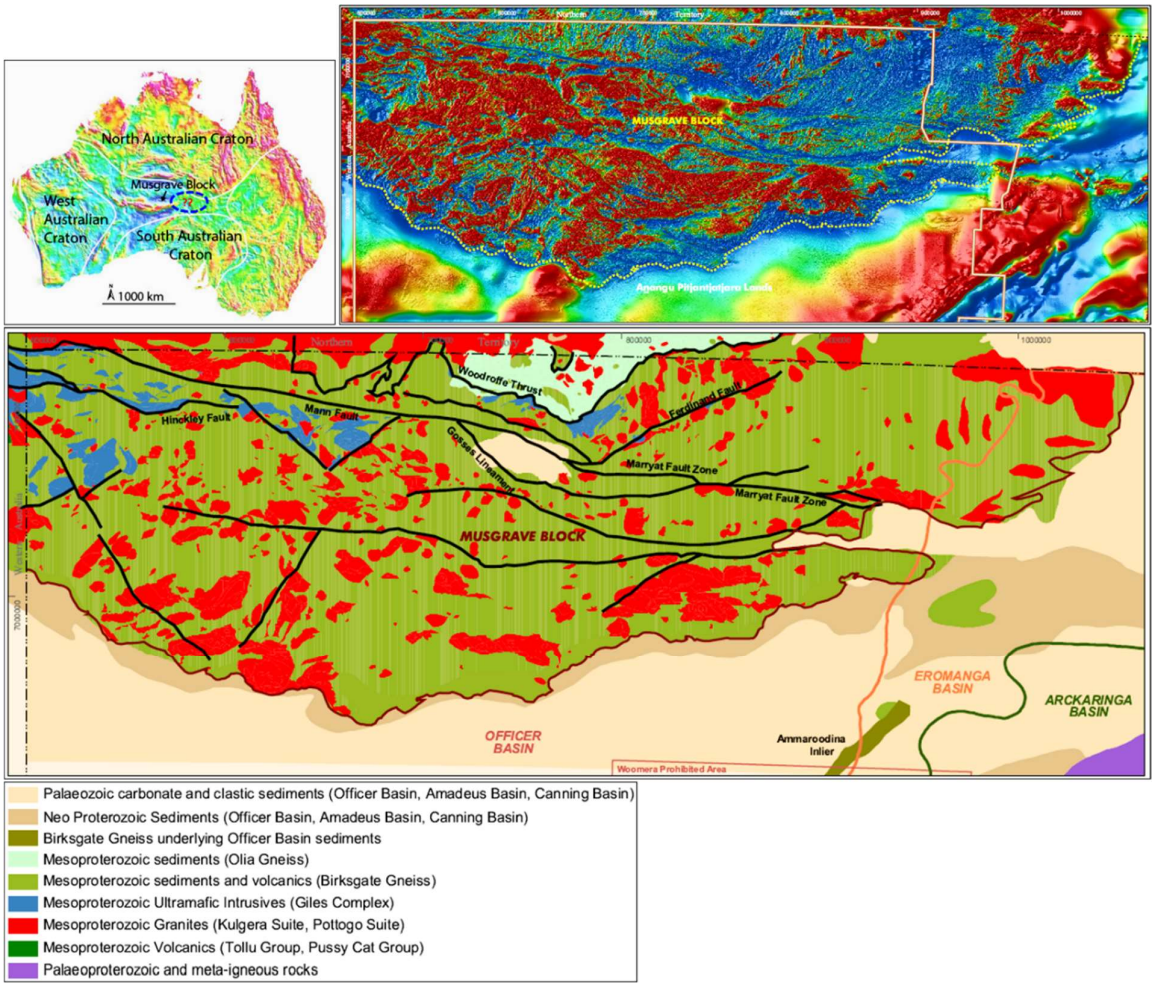

Figure 4. Mulga and Fregon Domains of the Musgrave Block in South Australia, from Woodhouse & Gum 2003 (TMI image and solid geology). Residual gravity anomaly map (top left) by Nakamura et al. (2011), craton boundaries and Tasman Line from Evins et al. (2010), adapted from Hawemann et al 2018.

2.3 Relevant minerals systems

Sandstone-hosted Uranium

The Upper Cretaceous Bulldog Shale and stratigraphically lower Coorikiana Sandstone of the Eromanga Basin cover EL 6458 (Figure 5). This area is moderately prospective for sandstone-hosted Uranium systems, which are typically small to medium tonnage (~ 40 MT @ 0.28% weight U, Jaireth et al 2015).

Further south, in the Callabonna Sub-basin (Frome Embayment), the Eyre Formation which stratigraphically overlays the marine transgressive Bulldog Shale hosts Australia's largest sandstone hosted uranium resources and insitu leaching operations: Beverley (16.3 kt U_3O_8), Honeymoon (2.9 kt @ 0.20 % U_3O_8) and Four Mile (13 kt @ 0.31% U_3O_8). The Four Mile West deposit is hosted in sands of the Bulldog Shale itself (19 kt @ 0.34 % U_3O_8). Together these resources account for 38% of

sandstone hosted uranium resources on the continent (McKay & Miezitis, 2001; Jaireth et al 2015, Figure 6).

There has been a strong historic focus on Sandstone-hosted Uranium on the Northern Territory side of the Central Australia Minerals Project, with explorers targeting a specific redox boundary in the Devonian Finke Group (Langra Formation) of the Amadeus Basin, and the Jurassic De Souza sandstone of the Eromanga Basin (CR1974.0028, 1974.0183).

Historic uranium explorers in the South Australian project area specifically targeted the Algebuckina Sandstone and the Bulldog Shale (ENV 3775, 3902).

There are two known uranium occurrences within the project area. The Curralulla occurrence is hosted in the Early Jurassic to Early Cretaceous Algebuckina Sandstone, while further south, the Enungarenna Hill occurrence is hosted in paleochannels within the Early Cretaceous Hooray Sandstone (both of the Eromanga Basin).

This mineral system requires inputs from surrounding felsic basement, such as the Mount Painter Inlier bordering the Callabonna sub-basin, meaning topography and fluid flow play a key role in the creation of this mineral system (Wilson 2015, Jaireth et al 2015).

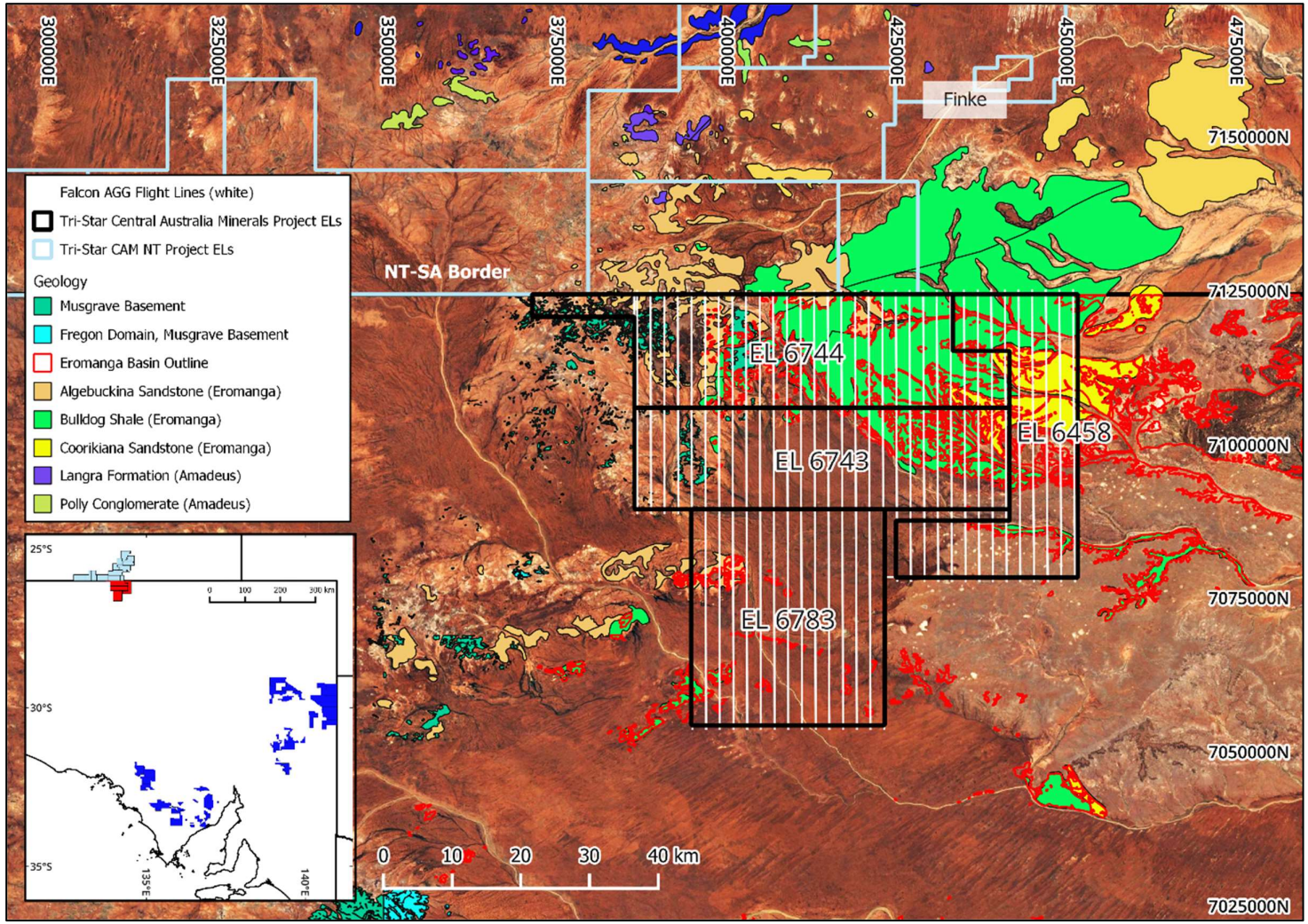

Figure 5. Geology of the Central Australia Minerals Project with Tertiary removed, showing Eromanga Basin and Musgrave Basement with AGG flight lines

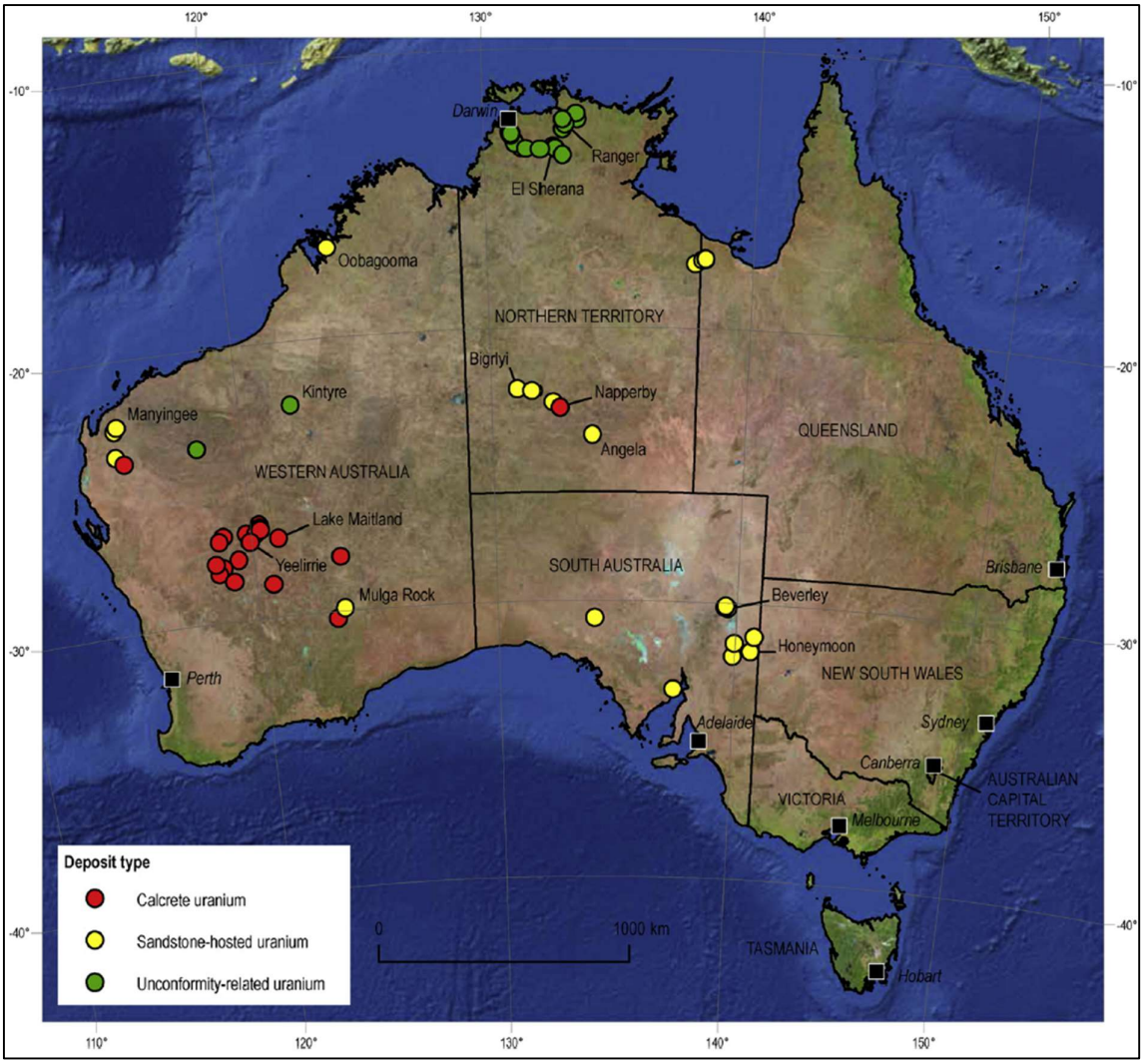

Figure 6. Broad style of uranium deposits in Australia showing the location of Beverley and Honeymoon resources in the Callabonna sub-basin of South Australia (from Jaireth et al 2015)

Orthomagmatic Ni-Cu ± PGE in ultramafic complexes

The Mesoproterozoic Musgraves Basement reached peak metamorphism (to granulite facies in the Fregon Domain) throughout the 1,090-1,040 Ma Giles Extensional Event. This event emplaced the 1,075 Ma Warakurna Large Igneous Province in the West-Central Musgrave as a series of fault-bound, layered intrusions (Wade et al 2008, Tucker et al 2012).

The Alcurra dolerite swarms mapped throughout the project area in both NT and SA are part of this event (Edgoose et al 1993, Close 2013), and the Abminga Bedrock Drilling Program (GSSA 2012) noted potential ultramafic rocks amidst the Birksgate granitic complex in the western portion of the licences (Tucker et al 2012, Figure 11).

In the western Musgraves, orthomagmatic nickel-copper-PGE resources such as Nebo-Babel occur in shallow (exhumed) conoliths offset from larger intrusive complexes (390 Mt @ 0.30% Ni, 0.33% Cu, 120 ppm Co, 0.06 g/t Au, 0.85 g/t Ag, 0.08 g/t Pt, 0.09 g/t Pd, OZ Minerals Reserves and Resources Statement 2022). Other prospects include Halleys Cu-PGE-Ni within a feeder zone for the ultramafic Saturn Intrusion, and Tollu copper area with mineralisation disseminated throughout gabbro and felsic volcanics (Woodhouse & Gum 2003; Joly et al 2014).

The Central Australia Minerals project area is prospective for these kind of resources, provided the basement lies within economically mineable depth of the surface.

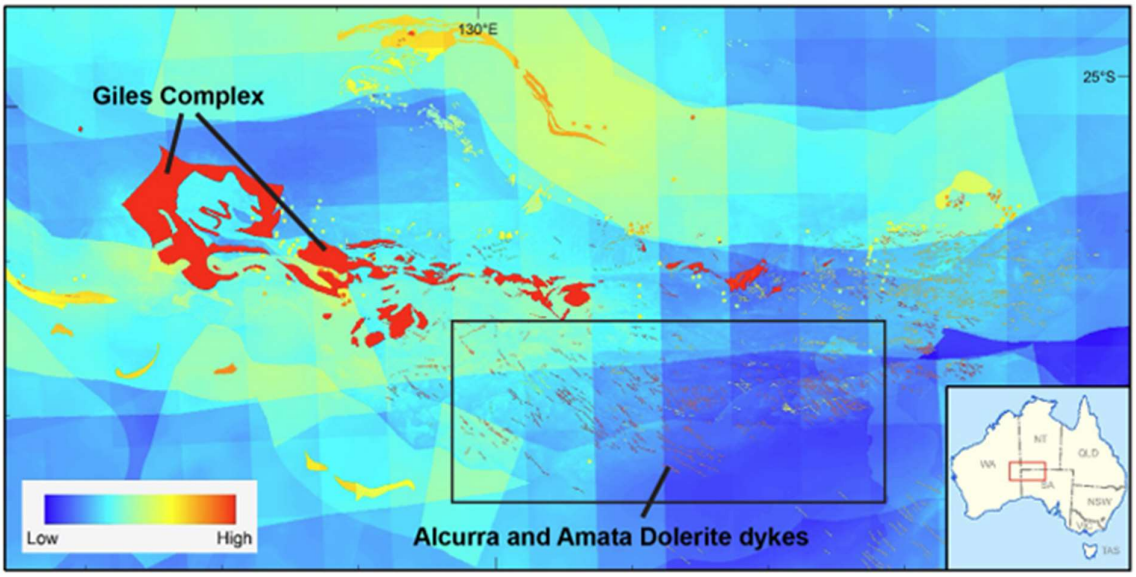

Figure 7. Expressions of the Giles Magmatic Event across the Musgraves showing the Alcurra Dolerites in the project area, from Dulfer et al 2016

2.4 Prior Exploration: Historic and Recent Work

Commodities sought by previous explorers in the Central Australia Minerals (CAM) project area include uranium in the Warburton-Amadeus, Pedirka and Eromanga Basins, diamonds in diatreme-like Musgravian basement features and base + precious metals of the Musgrave Giles Suite.

Spatial analysis of open file data shows that 26 different historic licence packages overlap with the current extents of the CAM Project. The most important on-ground work and insights relevant to the current project are discussed by commodity below.

Uranium (Eromanga Basin)

A number of companies with historic ELs overlapping the current project extents targeted sandstone-hosted Uranium in paleochannels where various units of the Eromanga Basin onlapped the crystalline basement of the Musgrave. These included Dampier Mining (EL 79 & 97 to 1974), Afmeco Ltd (ELs 574 & 653 to 1980), Eromanga Uranium (EL 3964 & 3982, 2008), Maximus Resources (ELs 3599, 3601 & 3602 to 2011), GE Resources (EL 4654 to 2013), Tychean Resources Ltd (ELs 3892 & 3964 to 2012) and Tianda Uranium (ELs 3873, 4493, 5233 & 5524 to 2014).

While a number of airborne surveys and hydrogeochemical sampling programs were undertaken by various explorers, the majority of historic drillholes in the project area were drilled by Afmeco Ltd and Eromanga Uranium (Figure 8).

Afmeco held a contiguous package of tenure extending into the Northern Territory. The company variably targeted the Crown Point Formation (the basal unit of the Pedirka Basin), and the Bulldog Shale, Algebuckina Sandstone and Canda-Owie Formations of the Eromanga Basin. They successfully delineated a paleochannel partially within the current project extents (drillholes CUR-1, and CUR-12 to 18). These drillholes intersected 'traces of radioactive minerals within economically discouraging lithological settings' (ENV 3775, 3902). The highest assay was CUR-13 (190 ppm U) on a redox front.

Eromanga Uranium held a package of contiguous ELs that stretched over 200km south from the Northern Territory border from 2008 to 2012. The company flew a REPTEM AEM-magnetic survey over the entire tenement package, and followed up paleochannels with a number of microgravity lines (ENV11775).

The company found that Mesozoic intervals comprising the Bulldog Shale and Coorikiana Sandstone recorded high conductivities relative to the Algebuckina Sandstone and post-Mesozoic strata. Conductive anomalies in favourable paleochannel positions were tested with aircore holes, using the shale as a stratigraphic marker. A number of these are in the south of the current project area (Figure 8).

The Eromanga Basin is overlain within the project area by the Stevenson Paleochannel and the Hamilton Basin (shown in Figure 14 and Figure 15). These are Pliocene (< 5 Ma) features. The sediments, consisting of '*poorly to well-sorted, silty and clayey, very fine to very coarse, feldspathic quartz sandstone with angular granules and pebbles of quartz, silcrete and claystone*' are interpreted as fluvial deposits laid down in flood-plain and piedmont fan environments (Drexel et al 1995).

There are no known uranium resources associated with this system, and the Stevenson Paleochannel presents as a radiometric uranium low, probably due to the superposition of the modern drainage system above it.

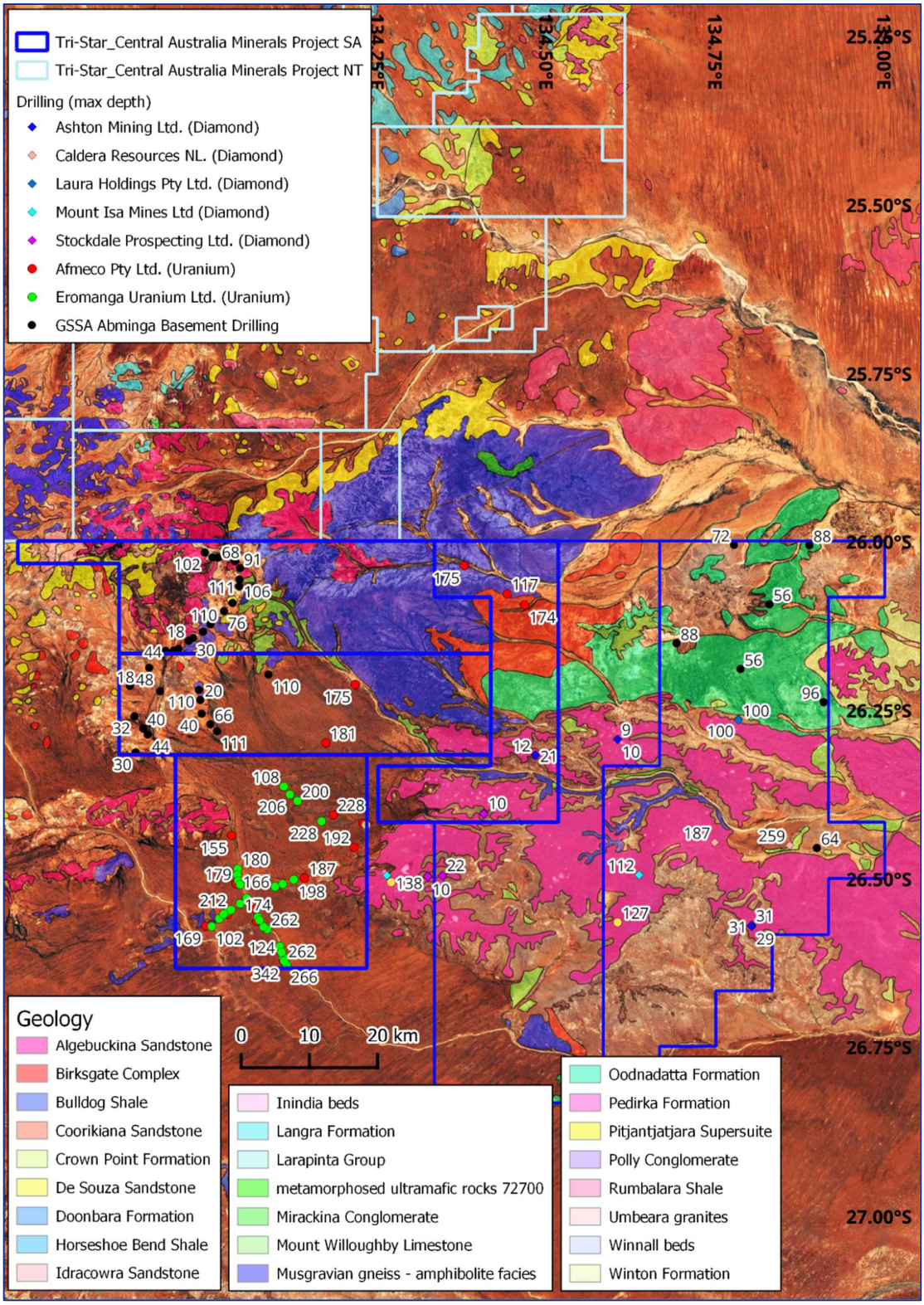

Figure 8. Historic drillholes by company and commodity shown over surface geology with Tertiary sand dunes removed

Diamonds (Musgrave Basement)

At the time that Argyle Diamond Mine was discovered in the Kimberley, it was understood that kimberlites occurred within stable, Proterozoic cratons while adjoining mobile zones were more likely to host lamproites (Woodhouse & Gum 2003). The age and tectonic setting of the Musgraves mobile belt fits the criteria for Argyle-type resources.

Caldera Resources operated the Abminga Diamond Project from 1993 to 2004 over a package of ELs that overlap with the central and southern portions of the current project (ENV9299, Figure 9). The company had various associations with other diamond explorers who also operated their own ELs, namely Eromanga Uranium Ltd, Laura Holdings/ Dioro Exploration NL (ELs 1916, 1917, 1918, 1934 & 2615), Stockdale Prospecting (De Beers, EL 1885), and Mount Isa Mines Ltd.

Other diamond explorers with overlapping ELs included Consolidated Diamonds (EL 1908) and Ashton Mining (EL 1882 & 1883).

Caldara Resources infilled the 400 m spaced SADME magnetic data at 100 m line spacing, then selected and prioritised a number of isolated, low amplitude, dipolar anomalies with short strike length that resembled diatremes (Figure 9).

Soil sampling for heavy minerals was done over a number of the targets, but results were inconclusive (ENV9299).

Of the 29 most prospective anomalies, seven were tested with aircore drilling in a JV with Mount Isa Mines in 1994. All the drill holes intersected the Bulldog Shale of the Eromanga Basin, described as siltstones and sandstones. More importantly, all the anomalies were explained by flat, thin, near-surface accumulation of maghemite on the Cretaceous unconformity surface (paleo depressions) rather than in the basement, with magnetic strengths measured from 20-500 SI.

The coincident, circular radiometric anomalies at surface were subsequently explained by Tertiary lake clays. No tuffaceous (diatreme) type sediments were seen in hand sample, nor through petrographic analysis (ENV9299, Figure 9).

In all, the companies above drilled 33 holes into bullseye magnetic anomalies, down to weathered basement but no tuffaceous sediments were ever intersected. Poor results were compounded by Native Title complications, and much of the ground was surrendered in the mid-2000s (summarised by Woodhouse & Gum 2003, Figure 8).

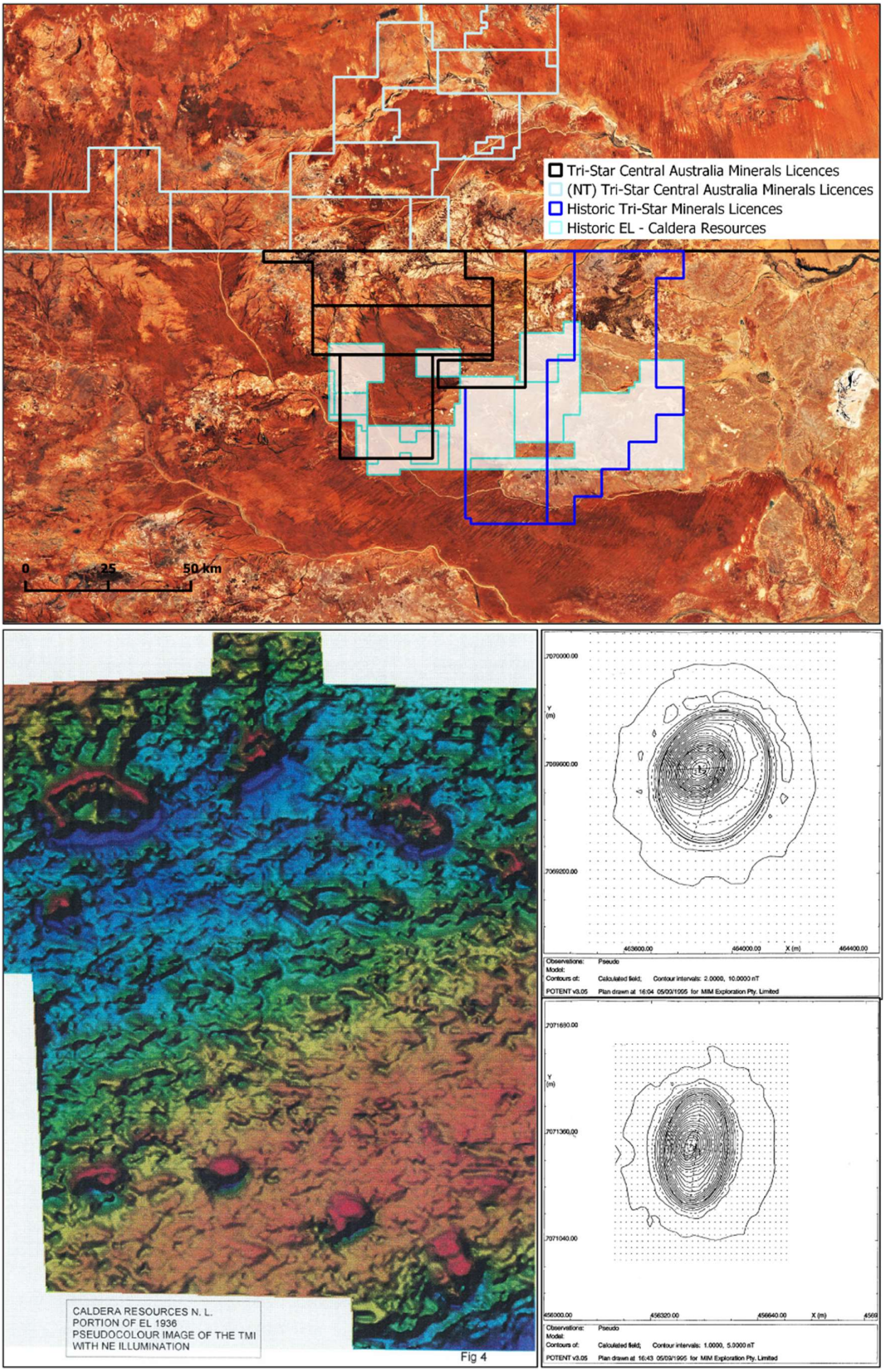

Figure 9. 100 m spaced magnetic (TMI) image and modelling of anomalies tested in the Abminga Diamond Project

Base and precious metals (Ni-Cu-PGE)

Some of the most informative data in the project area comes from the GSSA Abminga Bedrock Drilling Program (Tucker et al 2012). 30 drillholes of the 140-hole program fall within the current project extents.

To the west of the tenements, the drilling intersected ultramafics with visible sulphides, and elevated levels of Ni, Cu, Co, PGE and Au, leading to a number of targets pursued on EL 6090 adjacent to the current project area. The same program also intersected some silver-mineralised granites of the Birksgate Complex, with extreme enrichments in Eu and HREE probably related to hydrothermal sulphide mineralisation (Tucker et al 2012), raising the possibility of BHT targets.

Over the previous two decades, a number of explorers with adjacent or partially overlapping historic leases have targeted orthomagmatic nickel-copper in Giles-aged ultramafics including Goldsearch Ltd (EL 2910, operated by Independence Group from 2002 to 2007), Norsa Exploration Pty Ltd (ELs 5286, 5287 & 6180 to 2021), Swancove Enterprises Pty Ltd (ELs 4056 & 4061, to 2009) and Woomera Exploration Ltd (EL 6090, to 2021).

On EL 6090 adjacent to the western boundary of the current project area, Independence Group found that processing of the existing magnetic data was able to delineate near-surface Alcurra Dolerites cross-cutting older units of the Fregon Subdomain (Birksgate Gneiss). However, their reports note an absence of larger Giles Complex structures (such as the Saturn Intrusion of the West Musgraves) within the project area (ENV9885, Figure 10). The ground is now held by Rio Tinto Exploration.

Within the current project area, the GSSA drillholes confirmed the basement is a combination of the Birksgate Gneiss, intruded by the Kulgera Granites, with minor (Giles) ultramafic intrusives (Tucker et al 2012).

Drillholes with summary lithology are shown in Figure 11, with the solid geology units as mapped (Musgrave basement only). Despite the number of overlapping leases, there are no exploration drillholes within the current SA project extents testing for this mineralisation style.

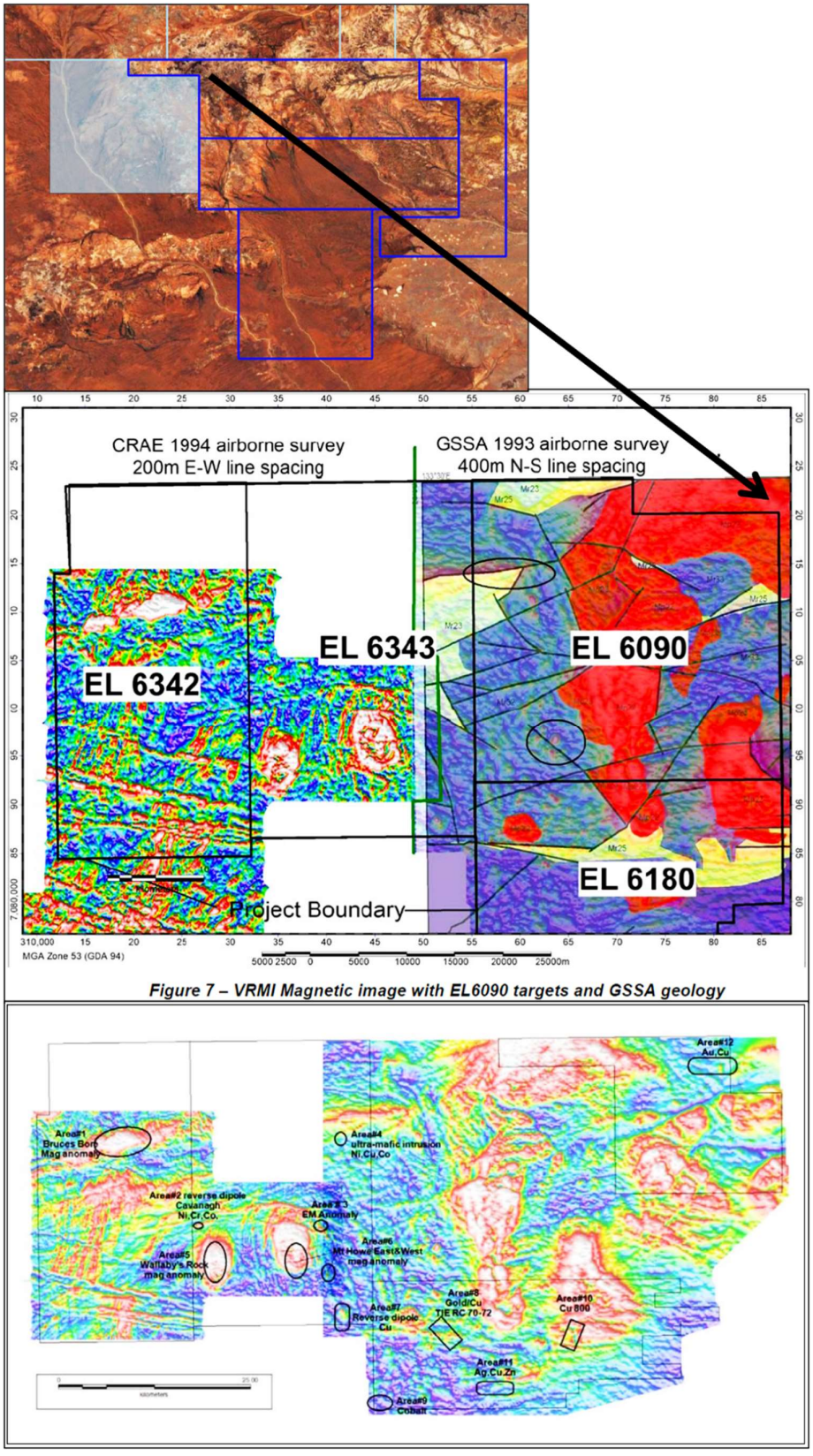

Figure 7 – VRMI Magnetic image with EL6090 targets and GSSA geology

Figure 10. Targets defined by Woomera Exploration from magnetic data and GSSA drilling results (ENV13166)

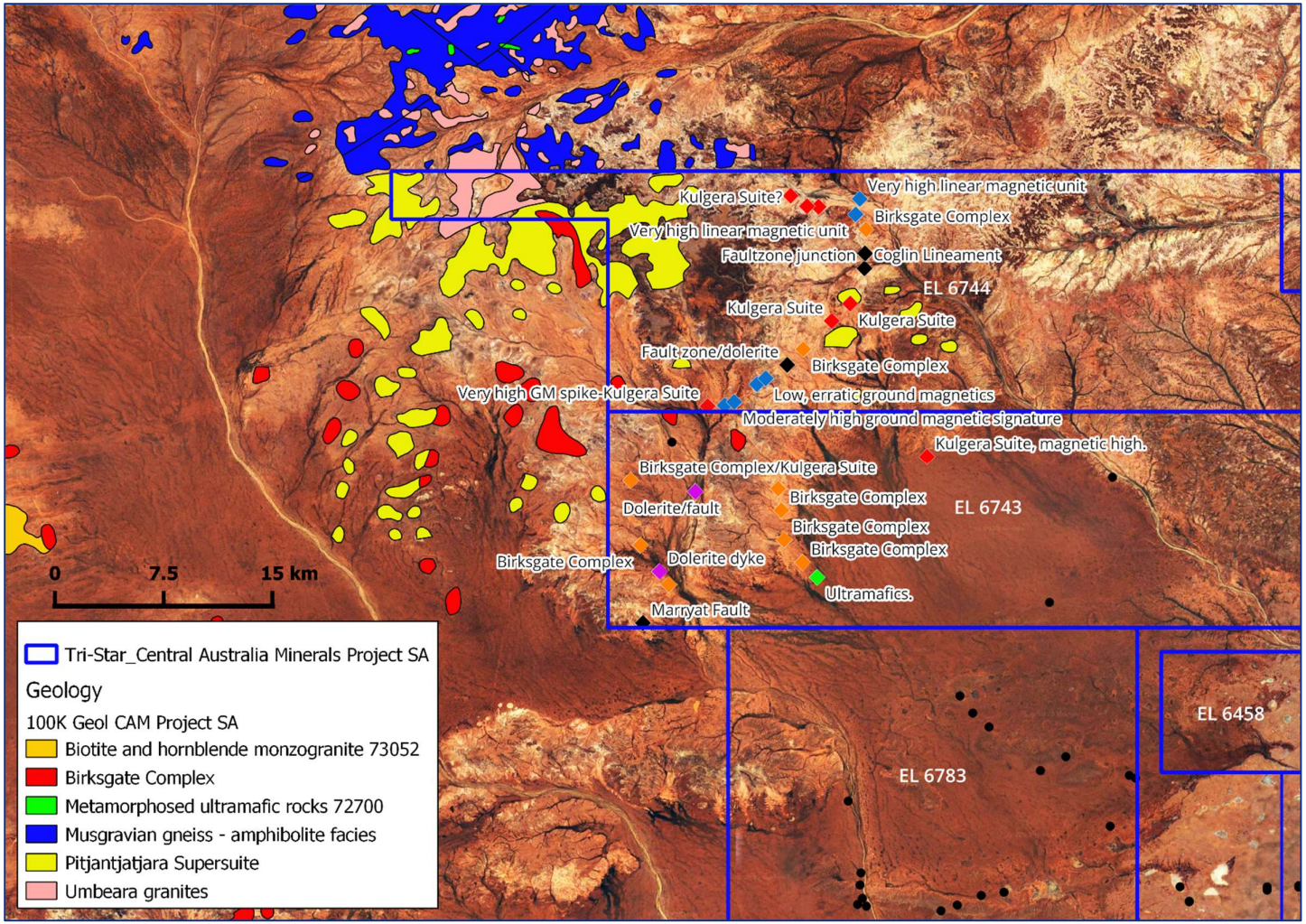

Figure 11. GSSA Ambinga Baserock Drilling Program holes with summary lithology shown with surface outcrops of Musgrave Basement

3. Exploration over the life of the tenure

3.1 Geophysics – airborne surveys (Survey data - see SARIG Website)

New data acquisition occurred in Year 2 of EL 6744. Tri-Star commissioned a 20,729 km Falcon® Airborne Gravity Gradiometery (AGG) survey flown by Xcalibur Multiphysics Pty Ltd.

The Central Australia Minerals Project flight area comprised 1,844 line kilometres at a minimum drape height of 80 m, at two-kilometre north-south spacing (179/ 359º). No tie lines were flown.

465 line km of this was flown within the original extents of EL 6743 & 480 line km over EL 6744.

The full logistics report from this survey is provided in Appendix 1, with flight lines shown in Figure 1 and Figure 2. Full AGG data and subsequent geophysical processing products were submitted to the Department with the AEA 051-001 Annual Activity Report (2024).

This portion of the semi-regional survey was flown in a series of five production flights from September 1st to 3rd, 2023 using Alice Springs as a base (GPS Base Station 23º 48' 03.73870" S/ 133º 53' 55.99593" E/ 558.504 m height ellipsoidal).

The survey produced data of excellent quality, with minor turbulence and no instrumental issues. No delays or incidents occurred, and data was received with full terrain correction. Specifically:

- Vertical Gravity (gD) with terrain corrections of 0 g/cm^3, 2.6 g/cm^3 and an additional value (2.1 g/cm^3) determined using the in-house Density Correlation Tool (generally a density of less than 2.67g/cm^3 is indicative of sediments / lower density granites).
- Vertical Gravity Conformed (gD conformed) with terrain corrections
- Vertical Gravity Gradient (gDD) with terrain corrections.

Geophysical processing and integration

The gravity data underwent inversion modelling to assist with depth determination and image major structures with information on size, dip and relative density. This was done by GeoDiscovery Ltd throughout February 2024.

The final airborne gravity data was gridded using a minimum curvature routine. gD 2.0 TC was used as input for the density models, input into the Geosoft Voxi inversion code and run as a sampled dataset. Model voxels of dimensions 270m x 270m (XY) and 135m thick (Z) over the entire survey regions were used down to a total depth of over 4000m. This output resolution is useful for interpretations of regional structures and identification of broad target regions.

High Pass Bouguer Anomaly gravity images and Tilt Derivatives were applied to the data. The high pass filtering attempts to remove the longer wavelength regional trend, in order to reveal localised (and shallower) features within the study region, such as the lower density paleochannels. The Tilt Derivative highlights edges, which can be indicative of geological boundaries and structures.

The AGG data was also integrated with the complete magnetic and radiometric coverage over the area, and the available AEM data. A number of preliminary targets were selected for further evaluation in the context of mapped solid geology and knowledge of the mineral systems.

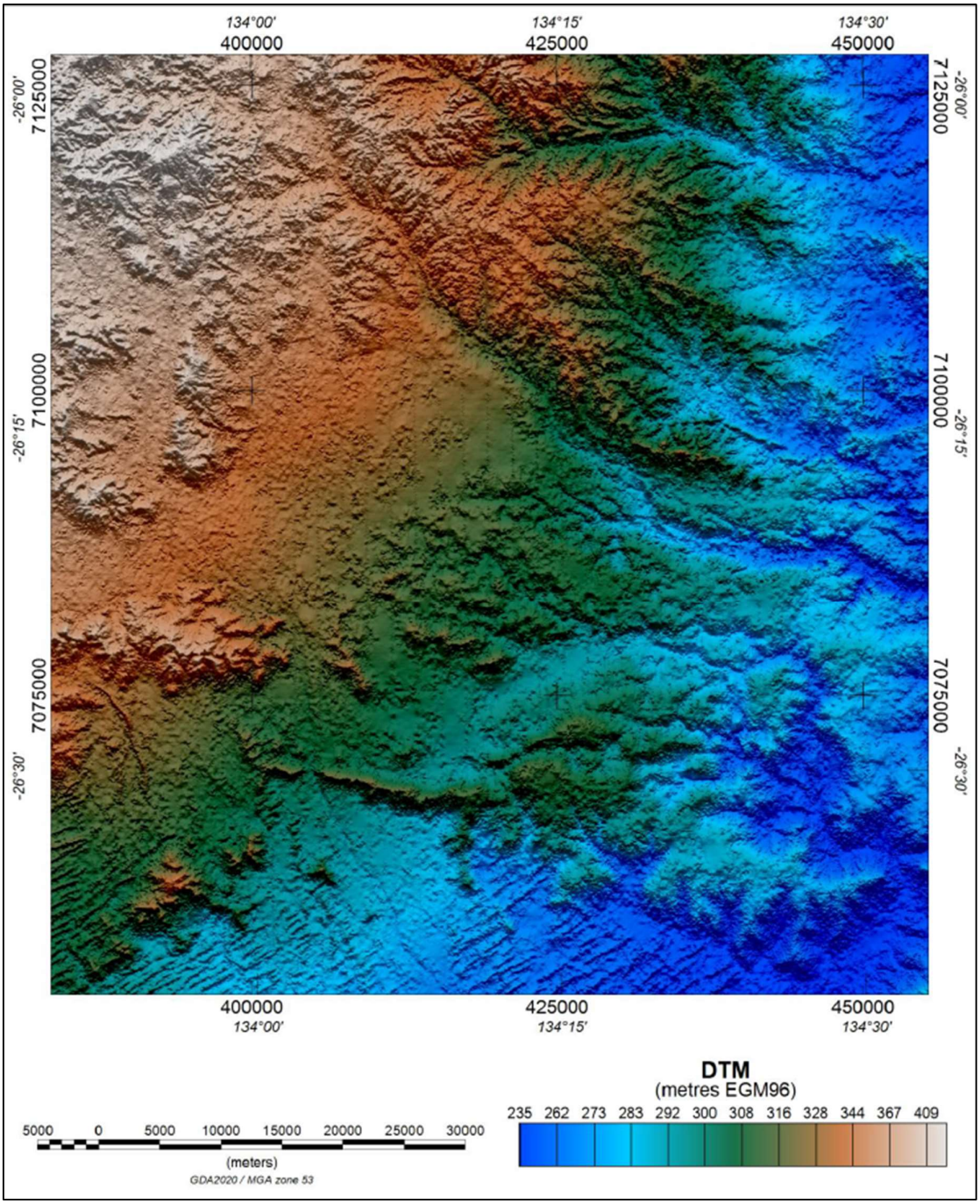

Figure 12. Digital elevation model produced from the Falcon AGG survey coupled with GA DEM-S data (Xcalibur Multiphysics logistics report)

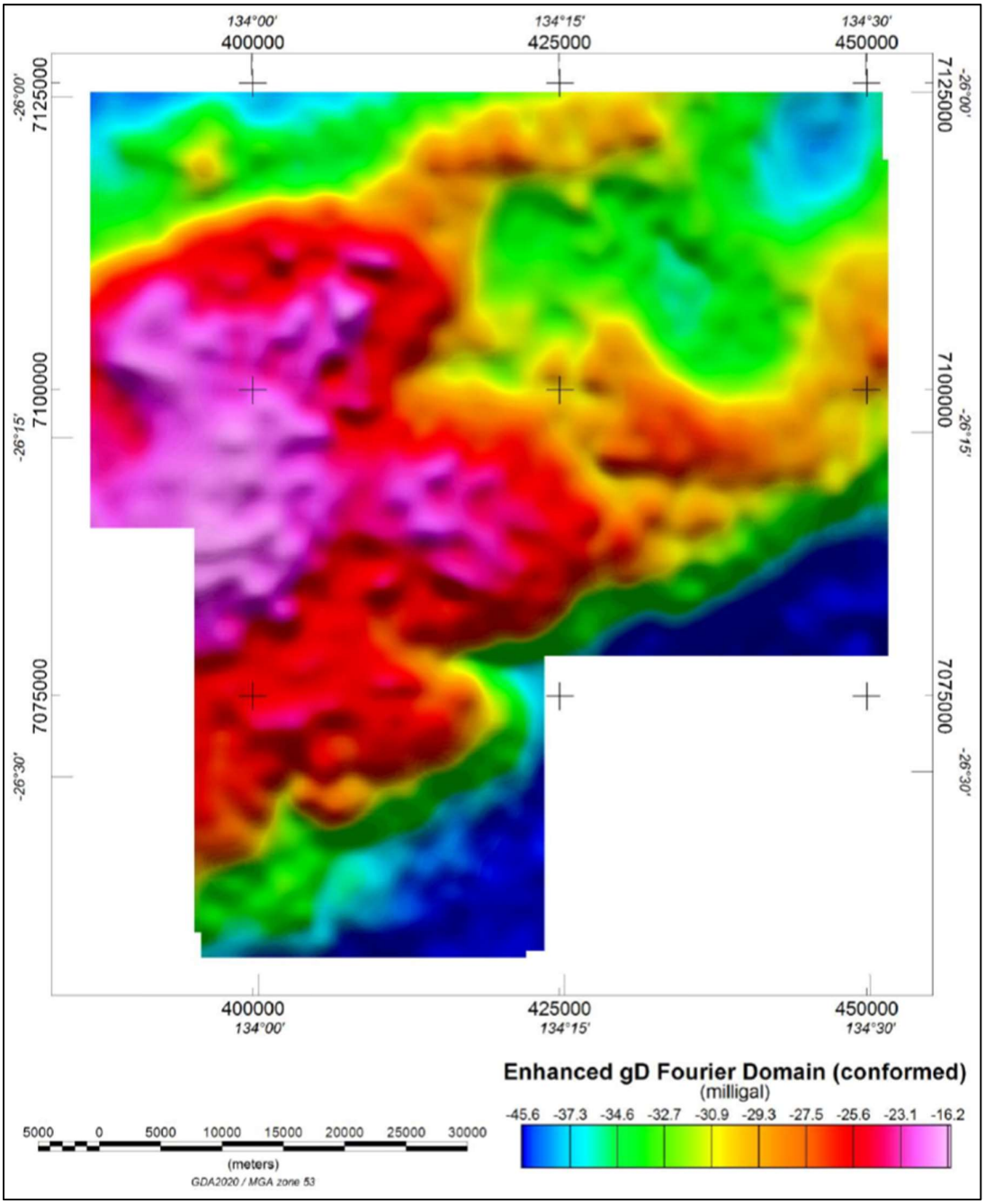

Figure 13. Enhanced Vertical Gravity (gD) from Fourier processing conformed to regional gravity data (milligal) from Xcalibur Multiphysics logistics report

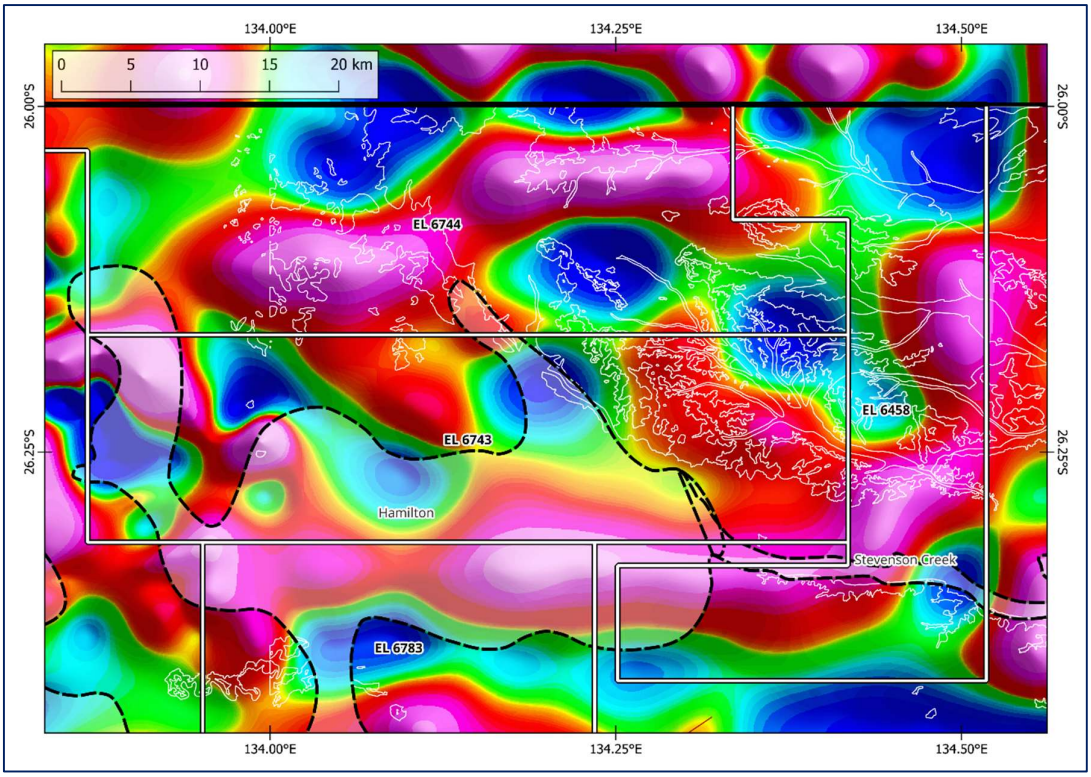

Figure 14. Original regional gravity resolution over the project area, showing the < 5 Ma Paleovalley features

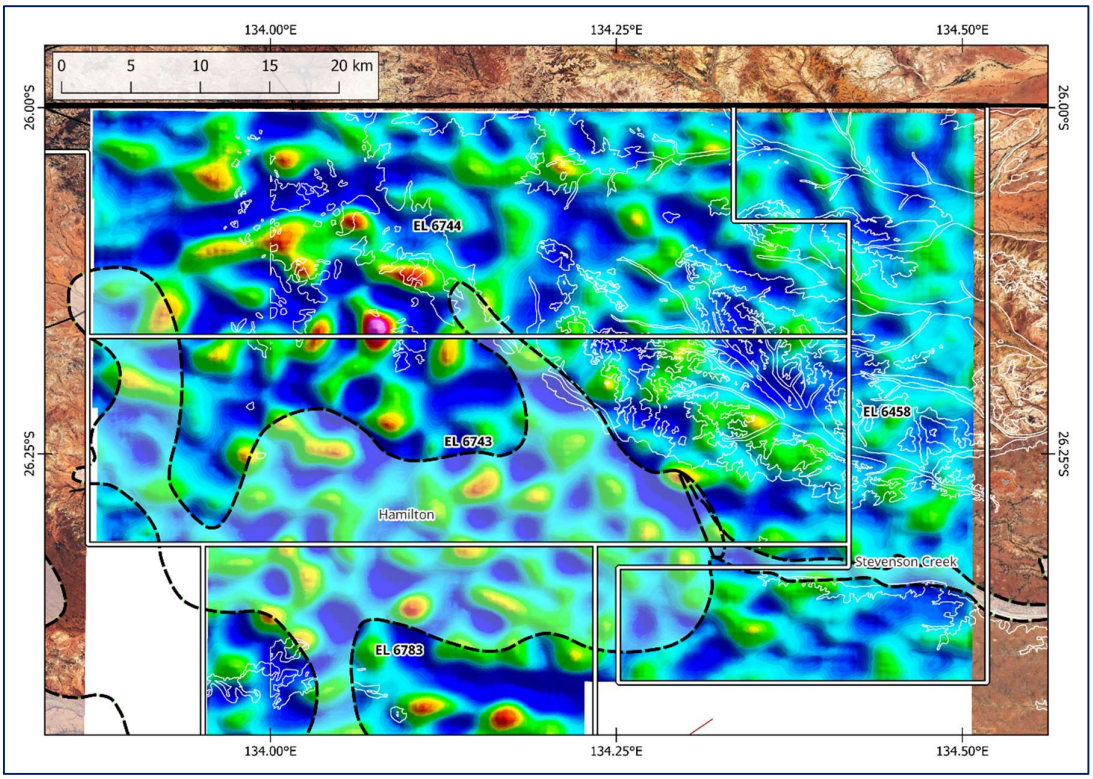

Figure 15. Falcon AGG density inversion 400m depth slice with linear stretch

3.2 Target generation, evaluation and rationale for surrender

Despite the underlying Musgraves basement being 250-550 m within the surrendered portion of the EL, there are no highly ranked targets identified in the reprocessed magnetic, radiometric, AEM data, nor the newly acquired AGG data (depth estimates constrained by drilling, GSSA, Figure 16).

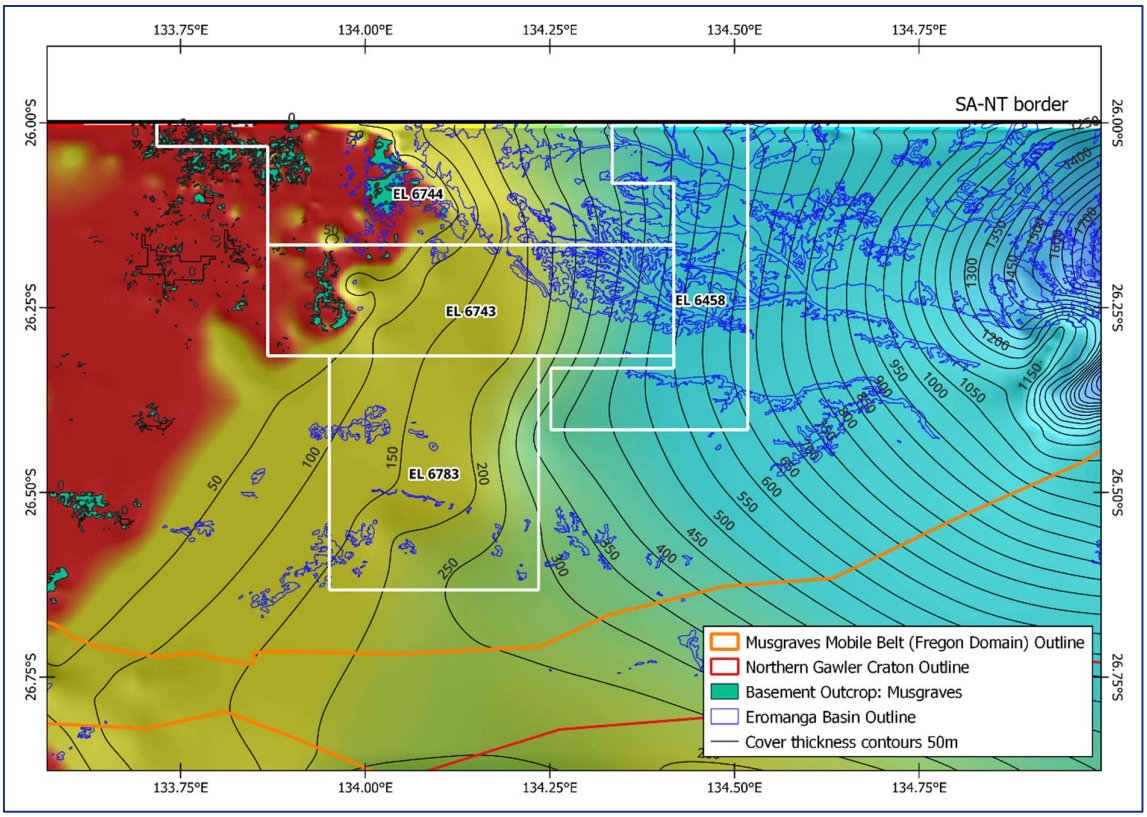

Figure 16. AEA 051-001 Central Australia Minerals current project extents shown with depth to basement contours and colour stretch (GSSA), Musgrave outcrops and inferred edge of the Musgraves Mobile Belt.

Conclusion

Work over the surrendered portions of EL 6743 & EL 6744 consisted of desktop data compilation and target generation work prior to the current year (ending July 2024), in which Tri-Star commissioned a regional Falcon Airborne Gravity Gradiometry (AGG) survey of 20,729 line kilometres. 945 line km of this was flown over the surrendered areas at 1 km north-south line spacing.

After the data was received, it was processed and integrated with existing geophysical datasets, and a comprehensive review of targets and company strategy followed. The survey returned high quality data enabling the identification of discrete targets and priority areas. It has also enabled the company to select a suitable area for relinquishment.

The survey will hopefully contribute to knowledge of the structure and solid geology of the Musgraves Fregon Domain in the future.

References

Aitken, A., Betts, P. & Ailleres, L. 2009. The architecture, kinematics, and lithospheric processes of a compressional intraplate orogen occurring under Gondwana assembly: The Petermann orogeny, central Australia. Lithosphere; v. 1; no. 6; p. 343–357.

Aitken, A & Betts, P. 2009a. Constraints on the Proterozoic supercontinent cycle from the structural evolution of the south-central Musgrave Province, Central Australia. Precambrian Research 168 (2009) 284–300.

Alexander, E. & Jensen-Schmidt, B. 1995. Eringa Trough Exploration Opportunity. Report Book 95/36, Petroleum Division, Mines and Energy South Australia.

Alghamdi, A., Aitken, A. & Dentith, M. 2018. The deep crustal structure of the Warakurna LIP, and insights on Proterozoic LIP processes and mineralization. Gondwana Research Volume 56, April 2018, Pages 1-11.

Ambrose GJ, 2006. Pedirka/Simpson Desert/Eromanga Basins: in Northern Territory of Australia, onshore hydrocarbon potential, 2006. Northern Territory Geological Survey, Record 2006-003.

Ambrose GJ & Heugh J. 2010. Petroleum geology of the Simpson Desert area: The Eromanga, Simpson, Pedirka and Warburton basins. Central Petroleum Ltd, internal report.

Ambrose GJ, Heugh J, Askin H & Alamiyo B. 2012. A Devonian rimmed carbonate platform complex and barrier reef complex offers new exploration opportunities in the Simpson Desert: in Ambrose GJ and Scott J (editors) 'Central Australian Basins Symposium (CABS) III'. Petroleum Exploration Society of Australia, Special Publication.

Ambrose GJ, Liu Keyu, Deighton I, Eadington PJ & Boreham CJ, 2002. New petroleum models in the Pedirka Basin, Northern Territory, Australia: in 'Australian Petroleum Production and Exploration Association conference, Adelaide, 21 – 24 April 2002'. APPEA Journal 42, 259 - 286.

Betts, P.G., Giles, D., 2006. The 1800–1100 Ma tectonic evolution of Australia. Precambrian Research 144, 92–125.

Carr, L. K., Korsch R. J., Palu T. J. and Reese, B. Onshore Basin Inventory: The McArthur, South Nicholson, Georgina, Wiso, Amadeus, Warburton, Cooper and Galilee basins, central Australia. Geoscience Australia Record 2016/04. Geoscience Australia, Canberra.

Close DF, 2013. Chapter 21: Musgrave Province: in Ahmad M and Munson TJ (compilers). 'Geology and mineral resources of the Northern Territory'. Northern Territory Geological Survey, Special Publication 5.

Cross, A.J., Dunkley, D.J., Bultitude, R.J., Brown, D.D., Purdy, D.J., Withnall, I.W., Von Gnielinski, F.E. & Blake, P.R., 2015. Summary of results joint GSQ-GA geochronology project: Thomson Orogen, New England Orogen and Mount Isa region, 2010–2012. *Queensland Geological Record*, 2015/01, 138 pp.

Drexel, J.F. and Preiss, W.V. (Eds), 1995. The geology of South Australia. Vol. 2, The Phanerozoic. South Australia. Geological Survey. Bulletin, 54.

Edgoose CJ. 2013. Chapter 23: Amadeus Basin: in Ahmad M and Munson TJ (compilers). 'Geology and mineral resources of the Northern Territory'. Northern Territory Geological Survey, Special Publication 5.

Edgoose CJ and Munson TJ, 2013. Chapter 34: Warburton Basin: in Ahmad M and Munson TJ (compilers). 'Geology and mineral resources of the Northern Territory'. Northern Territory Geological Survey, Special Publication 5.

Hawemann, F., Mancktelow, N.S., Pennacchioni, G., Wex, S. & Camacho, A., 2019. Weak and slow, strong and fast: How shear zones evolve in a dry continental crust (Musgrave Ranges, Central Australia). Journal of Geophysical Research: Solid Earth, 124(1), pp.219-240.

Hibburt, J.E. and Gravestock, D.I., 1995. Pedirka Basin. The geology of South Australia, 2, pp.88-90.

Jarrett A, Edwards D, Boreham, C & McKirdy, D. 2016. Petroleum geochemistry of the Amadeus Basin. AGES 2016 Proceedings, NT Geological Survey.

Joly, A, Aitken, ARA, Dentith, MC, Porwal, A, Smithies, RH and Tyler, IM 2014, Mineral systems analysis of the west Musgrave Province: regional structure and prospectivity modelling: Geological Survey of Western Australia, Report 117, 99p.

McKay, A.D., Miezitis, Y., 2001. Australia's uranium resources, geology and development of deposits. AGSO-Geoscience Australia, Mineral Resource Report 1, p. 195.

Munson TJ, 2013. Chapter 41: Eromanga Basin: in Ahmad M and Munson TJ (compilers). 'Geology and mineral resources of the Northern Territory'. Northern Territory Geological Survey, Special Publication 5.

Munson TJ & Ahmad M. 2013. Chapter 38: Pedirka Basin: in Ahmad M and Munson TJ (compilers). 'Geology and mineral resources of the Northern Territory'. Northern Territory Geological Survey, Special Publication 5.

Northern Territory Geological Survey. 2017. Overview of known conventional and unconventional petroleum potential in the Northern Territory Information brief for the Scientific Inquiry into Hydraulic Fracturing in the Northern Territory. NT Fracking Inquiry 2017.

Purdy, D.J., Carr, P.A. & Brown, D.D., 2013. A review of the geology, mineralisation, and geothermal energy potential of the Thomson Orogen in Queensland. Queensland Geological Record, 2013/01, 212 pp.

Smithies, R., Howard, H., Evins, P., Kirkland, C., Bodorkos, S. & Wingate, M. 2008. The west Musgrave Complex - new geological insights from recent mapping, geochronology, and geochemical studies: Geological Survey of Western Australia, Record 2008/19, 20p.

Smyth, M. & Saxby, JD. 1981. Organic petrology and geochemistry of source rocks in the Pedirka-Simpson Basins Central Australia. The APPEA Journal, 21(1), pp.187-199.

Subhash Jaireth, Ian C. Roach ∗, Evgeniy Bastrakov, Songfa Liu. Basin-related uranium mineral systems in Australia: A review of critical features. Ore Geology Reviews 76 (2015) 360–394

Tucker N, Gum J, Constable S and Dutch R 2012. Abminga bedrock drilling program 2001, Report Book 2012/00008. Department for Manufacturing, Innovation, Trade, Resources and Energy, South Australia, Adelaide.

Wade, B.P., Kelsey, D.E., Hand, M., Barovich, K.M., 2008. The Musgrave Province; stitching North, West and South Australia. Precambrian Research 166 (1–4), 370–386.

Walter MR, Veevers, JJ, Calver CR and Grey K, 1995: Neoproterozoic stratigraphy of the Centralian Superbasin, Australia. Precambrian Research

Walters, S. G. (1996). Broken Hill Type Pb-Zn-Ag deposits, geological characteristics and exploration models. CODES Master of economic Geology Course Manual 4, University of Tasmania.

Wilson T 2015. Uranium and uranium mineral systems in South Australia – Third edition, Report Book 2015/00011. Department of State Development, South Australia, Adelaide.

Woodhouse, A. & Gum, J., 2003. Musgrave Province — geological summary and exploration history. South Australia. Department of Primary Industries and Resources. Report Book, 2003/21.

Company Reports

Northern Territory

CR1974.0028, https://geoscience.nt.gov.au/gemis/ntgsjspui/simple-search?query=EL745

CR1974.0183, https://geoscience.nt.gov.au/gemis/ntgsjspui/simple-search?query=EL746

South Australia

https://sarigbasis.pir.sa.gov.au/WebtopEw/ws/samref/sarig1/cat0/MSearch

ENV3775 (Afmeco Pty Ltd)

ENV3902 (Afmeco Pty Ltd)

ENV9299 (Caldera Resources NL, MIM Exploration Pty Ltd and Astro Mining NL)

ENV9885 (Minex Australia Pty Ltd and Mithril Resources Ltd)

ENV11775 (Eromanga Uranium Ltd / ERO Mining Ltd)

ENV13166 (Woomera Exploration)

Appendix 1

EL6743 & EL6744 Partial Surrender Report_2024_P_02 Appendix 1

XCalibur Multiphysics Pty Ltd Falcon AGG Logistics Report

**Please note, the raw AGG data was submitted to the Department in full prior to this reporting deadline.*

(Survey data - see SARIG Website)

Tri-Star OPCO Pty Ltd

FALCON® Airborne Gravity Gradiometer Survey

Central Australia Minerals (Area 1), South Australia

Project Number: 2305051

Logistics and Processing Report

Xcalibur Aviation (Australia) Pty Ltd
Hanger 106, 10 Compass Road
Jandakot, Western Australia, 6164
AUSTRALIA

Xcalibur MULTIPHYSICS

Exploring the world
Safer, Clearer, Better

Table of contents

1 INTRODUCTION 5
1.1 Survey Location 5
1.2 General Disclaimer 6
2 SUMMARY OF SURVEY PARAMETERS 7
2.1 Survey Area Specifications 7
2.2 Data Recording 7
2.3 Project Safety Plan, HSE Summary 7
3 FIELD OPERATIONS 8
3.1 Operations 8
3.2 Base Stations 8
3.2.1 GPS Base Station (Javad Triumph-1) 8
3.3 Personnel 8
4 QUALITY CONTROL RESULTS 9
4.1 Survey acquisition issues 9
4.2 Flight Path Map 9
4.3 Turbulence 10
4.4 AGG System Noise 11
4.5 Digital Terrain Model 13
4.6 Drape Surface Deviation 15
5 FALCON® AIRBORNE GRAVITY GRADIENT (AGG) RESULTS 16
5.1 Processing Summary 16
5.2 FALCON® Airborne Gravity Gradiometer Data 16
5.3 Radar Altimeter Data 16
5.4 Laser Scanner Data 17
5.5 Positional Data 17
5.6 Terrain Correction 17
5.7 Regional Levelling 17
5.8 Enhanced Processing 17
5.9 FALCON® Airborne Gravity Gradient Data - G_{DD} & g_D 17
5.9.1 Fourier Transformation 17
5.9.2 Drape Surface 18
5.10 Conforming to regional gravity 20
6 APPENDIX I - SURVEY EQUIPMENT 21
6.1 Survey Aircraft 21
6.2 FALCON® Airborne Gravity Gradiometer 21
6.3 Airborne Data Acquisition Systems 21
6.4 Real-Time Differential GPS 21
6.5 GPS Base Station Receiver 21
6.6 Altimeter 21
6.7 Laser Scanner 21
6.8 Data Processing Hardware and Software 22

7 APPENDIX II - SYSTEM TESTS 23
7.1 Instrumentation Lag 23
7.2 Radar Altimeter Calibration 23
7.3 FALCON® AGG Noise Measurement 23
7.4 Daily Calibrations and checks 23
7.4.1 FALCON® AGG Quiescent Noise Check 23
7.4.2 FALCON® AGG Calibration 23
8 APPENDIX III - FALCON® AGG DATA & PROCESSING 24
8.1 Nomenclature 24
8.2 Units 24
8.3 FALCON® Airborne Gravity Gradiometer Surveys 24
8.4 Gravity Data Processing 24
8.5 Aircraft Dynamic Corrections 24
8.6 Self-gradient Corrections 25
8.7 Laser Scanner Processing 25
8.8 Terrain Corrections 25
8.9 Regional Levelling 25
8.10 Transformation into GDD & g_D 25
8.11 Terrain Corrections Using Alternate Terrain Densities 26
8.12 Noise & Signal 26
8.13 Risk Criteria in Interpretation 26
8.14 References 27
9 APPENDIX IV - FINAL PRODUCTS 28

Figures

Figure 1: Central Australia Minerals – Survey Area Location 5
Figure 2: Central Australia Minerals – Flight Path map 9
Figure 3: Central Australia Minerals – Turbulence (milli g where g = 9.80665 m/sec/sec) 10
Figure 4: Central Australia Minerals – System Noise NE (eotvos) 11
Figure 5: Central Australia Minerals – System Noise UV (eotvos) 12
Figure 6: Central Australia Minerals – Final Digital Terrain Model (metres, referenced to the EGM96 geoid) 14
Figure 7: Central Australia Minerals – Deviation from drape surface (metres) 15
Figure 8: FALCON® AGG Data Processing 16
Figure 9: Central Australia Minerals – Enhanced Vertical Gravity Gradient (GDD) from Fourier processing (eotvos). 18
Figure 10: Central Australia Minerals – Enhanced Vertical Gravity (gD) from Fourier processing (milligal) 19
Figure 11: Central Australia Minerals – Enhanced Vertical Gravity (gD) from Fourier processing conformed to regional gravity data (milligal) 20

Tables

Table 1: Survey Area Names 5
Table 2: Central Australia Minerals – Specifications 7
Table 3: Central Australia Minerals – Survey Boundary Coordinates 7
Table 4: Central Australia Minerals – Personnel 8
Table 5: Final FALCON® AGG Digital Data – ASEG GDF-II (ASCII) format 30
Table 6: Final FALCON® AGG Grids – ERMapper format 31

1 INTRODUCTION

Xcalibur Multiphysics conducted a high-sensitivity **FALCON®** Airborne Gravity Gradiometer (AGG) survey for the South Australian AGG Survey Areas under contract with Tri-Star OPCO Pty Ltd. There were ten areas flown, this report is for the **Central Australia Minerals** area.

Area name	Area number
Central Australia Minerals	1
Kimba	2
Kimba	3
Kimba	4
Whyalla	5
Whyalla	6
Frome South	7
Frome South	8
Strzelecki	9
Frome North	10

Table 1: Survey Area Names

1.1 Survey Location

The Central Australia Minerals survey area is centred on longitude 134° 12’ E, latitude 26º 19’ S (see the location map in *Figure 1*). The production flights took place during September 2023 with the first production flight taking place on September 1st and the final flight taking place on September 3rd. To complete the survey area coverage a total of 5 production flights were flown.

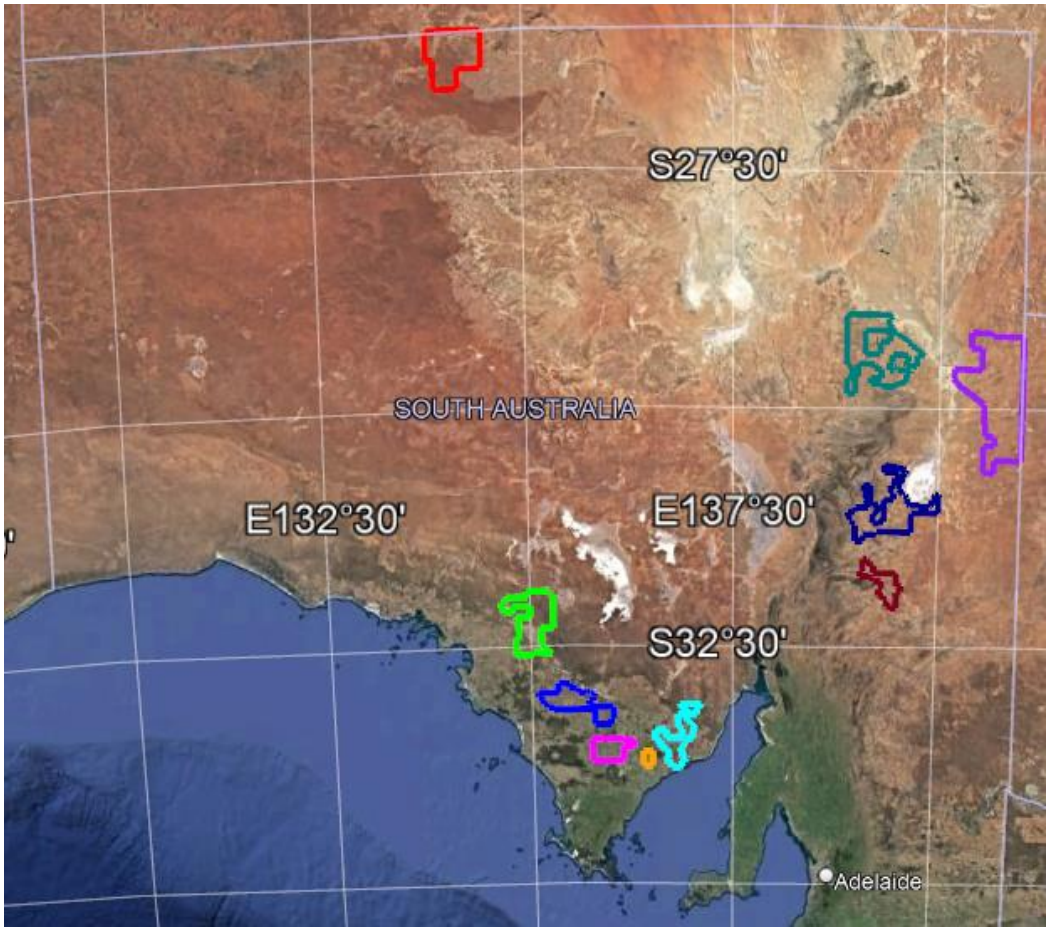

Figure 1: Central Australia Minerals – Survey Area Location

1.2 General Disclaimer

It is Xcalibur Multiphysics' understanding that the data and report provided to the Client are to be used for the purpose agreed between the parties. That purpose was a significant factor in determining the scope and level of the Services being offered to the Client. Should the purpose for which the data and report are used change, the data and report may no longer be valid or appropriate and any further use of, or reliance upon, the data and report in those circumstances by the Client without Xcalibur Multiphysics' review and advice shall be at the Client's own and sole risk.

The Services were performed by Xcalibur Multiphysics exclusively for the purposes of the Client. Should the data and report be made available in whole or part to any third party, and such party relies thereon, that party does so wholly at its own and sole risk and Xcalibur Multiphysics disclaims any liability to such party.

Where the Services have involved Xcalibur Multiphysics' use of any information provided by the Client or third parties, upon which Xcalibur Multiphysics was reasonably entitled to rely, then the Services are limited by the accuracy of such information. Xcalibur Multiphysics is not liable for any inaccuracies (including any incompleteness) in the said information, save as otherwise provided in the terms of the contract between the Client and Xcalibur Multiphysics.

2 SUMMARY OF SURVEY PARAMETERS

2.1 Survey Area Specifications

Total Kilometres (km)	1,876
Clearance Method	Drape
Minimum Drape Height (m)	80
Traverse Line Direction (deg.)	179 / 359
Traverse Line Spacing (m)	2,000
Tie Lines	None flown

Table 2: Central Australia Minerals – Specifications

The survey block is defined by the coordinates in *Table 3*, in UTM Zone 53S projection, referenced to the WGS84 datum.

Id	Easting	Northing
1	386655	7123920
2	451758	7124390
3	451930	7078245
4	423663	7078155
5	423818	7054110
6	395614	7053910
7	395327	7088984
8	387009	7088914

Table 3: Central Australia Minerals – Survey Boundary Coordinates

2.2 Data Recording

The following parameters were recorded during the course of the survey:

- **FALCON® AGG data:** recorded at different intervals.
- **Airborne GPS positional data** (latitude, longitude, height, time and raw range from each satellite being tracked): recorded at intervals of 1 s.
- **Terrain clearance:** provided by the radar altimeter at intervals of 0.1 s.
- **Time markers:** in digital data.
- **Ground based GPS positional data** (latitude, longitude, height, time and raw range from each satellite being tracked): recorded at intervals of 1 s.
- **Ground surface below aircraft:** mapped by the laser scanner system (when within range of the instrument and in the absence of thick vegetation), scanning at 36 times per second, recording 276 returns per scan.

2.3 Project Safety Plan, HSE Summary

A Job Safety Plan and Job Safety Analysis was prepared and implemented in accordance with the Xcalibur Multiphysics Occupational Safety and Health Management System.

3 FIELD OPERATIONS

3.1 Operations

The survey was based out of Alice Springs, Northern Territory. The survey aircraft was operated from Alice Springs Airport using aviation fuel available on site. A temporary office was set up in Alice Springs where all survey operations were run, and the post-flight data verification was performed.

3.2 Base Stations

A dual frequency GPS base station was set up in order to correct the raw GPS data collected in the aircraft.

3.2.1 GPS Base Station (Javad Triumph-1)

Location:	Alice Springs Airport
Date:	August 31st, 2023
Latitude:	23º 48' 03.73870" S
Longitude:	133º 53' 55.99593" E
Height:	558.504 m ellipsoidal

3.3 Personnel

The following technical personnel participated in survey operations:

Crew Leader:	V. Velu
Pilots:	N. Bowe, S. Fabig, P. Bouwer
Technicians:	V. Velu
Project Manager:	P. Johnson
QC and Processing:	C. Harmelin, M. Abubaker, P. Chambers

Table 4: Central Australia Minerals – Personnel

4 QUALITY CONTROL RESULTS

4.1 Survey acquisition issues

During the course of the survey, there were no data quality issues with:

- AGG instrumentation
- Data acquisition systems
- Radar altimeter
- Laser scanner

4.2 Flight Path Map

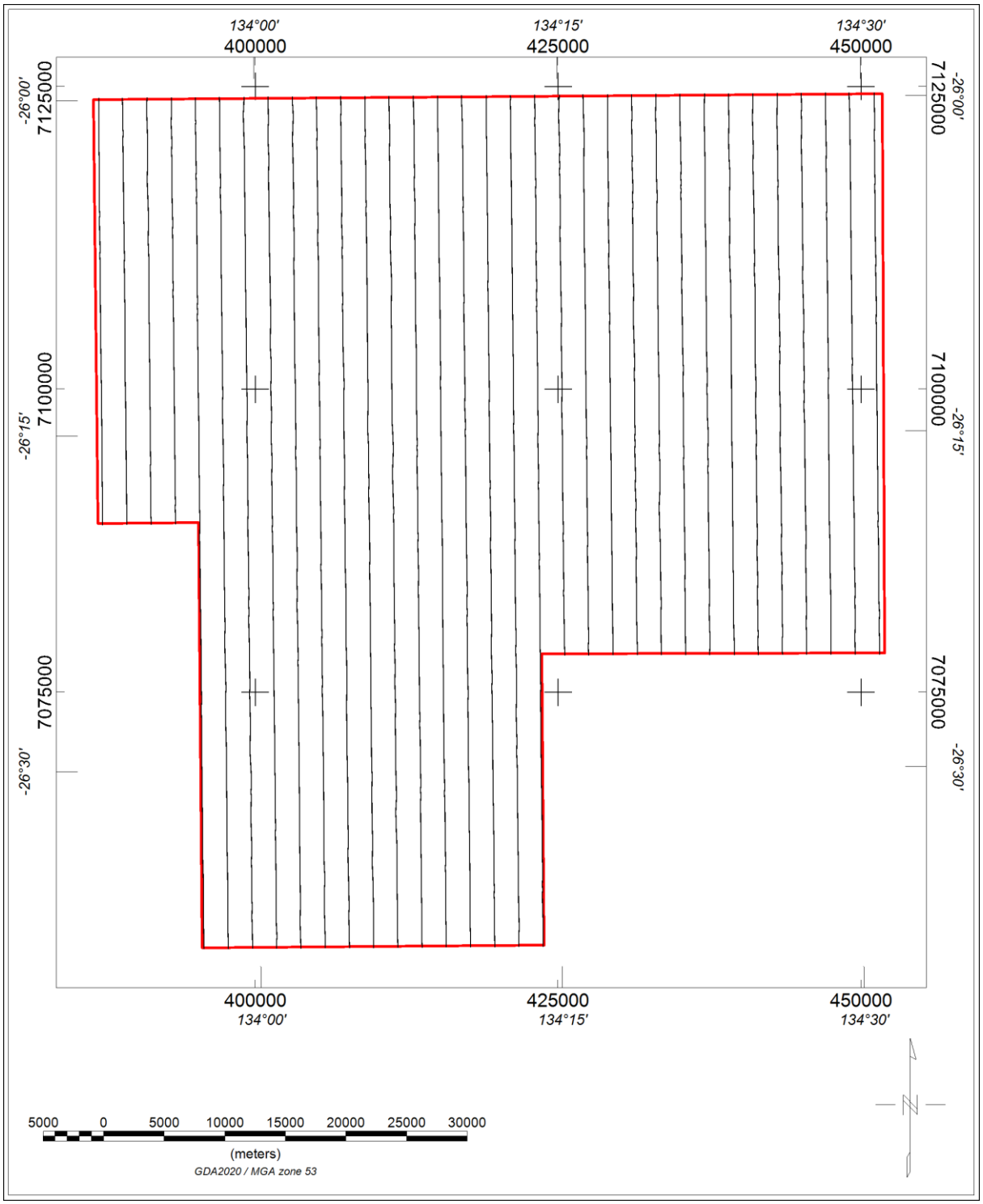

Figure 2: Central Australia Minerals – Flight Path map

4.3 Turbulence

The mean turbulence recorded in the Central Australia Minerals survey area was 66 milli g (where g = 9.80665 m/sec/sec). Turbulence was variable, ranging from very low to high. The typical pattern for a given day was for turbulence to increase and decrease with daily temperature. The turbulence pattern across the survey area is shown in *Figure 3*.

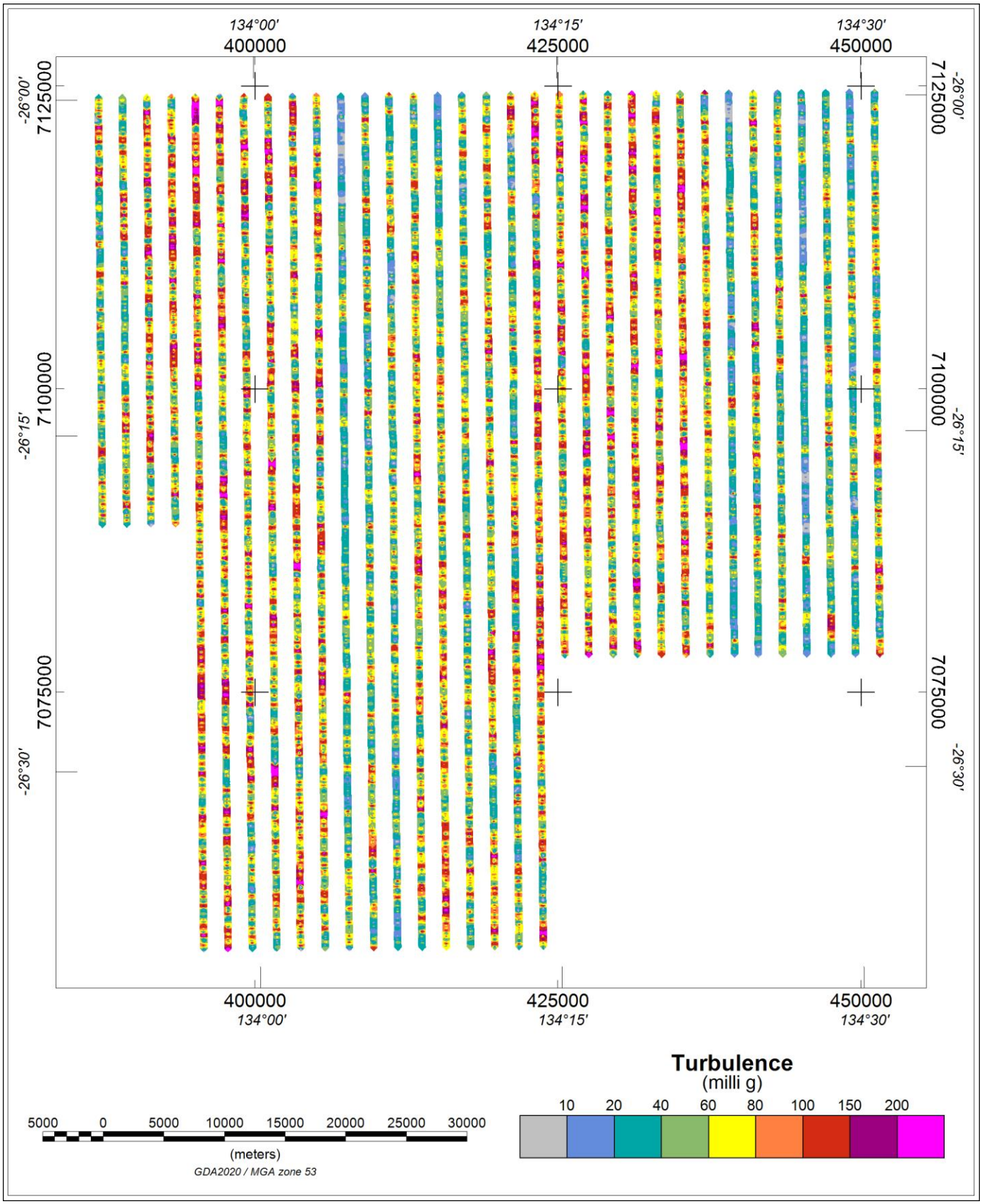

Figure 3: Central Australia Minerals – Turbulence (milli g where g = 9.80665 m/sec/sec)

4.4 AGG System Noise

The system noise is defined to be the standard deviation of half the difference between the A & B complements, for each of the NE and UV curvature components. The results for this survey were very good with values of 2.80 E and 2.79 E for NE and UV respectively.

Figure 4 and *Figure 5* provide a representation of the variation in this standard deviation for each component. This is achieved by gridding a rolling measurement of standard deviation along each line using a window length of 100 data points.

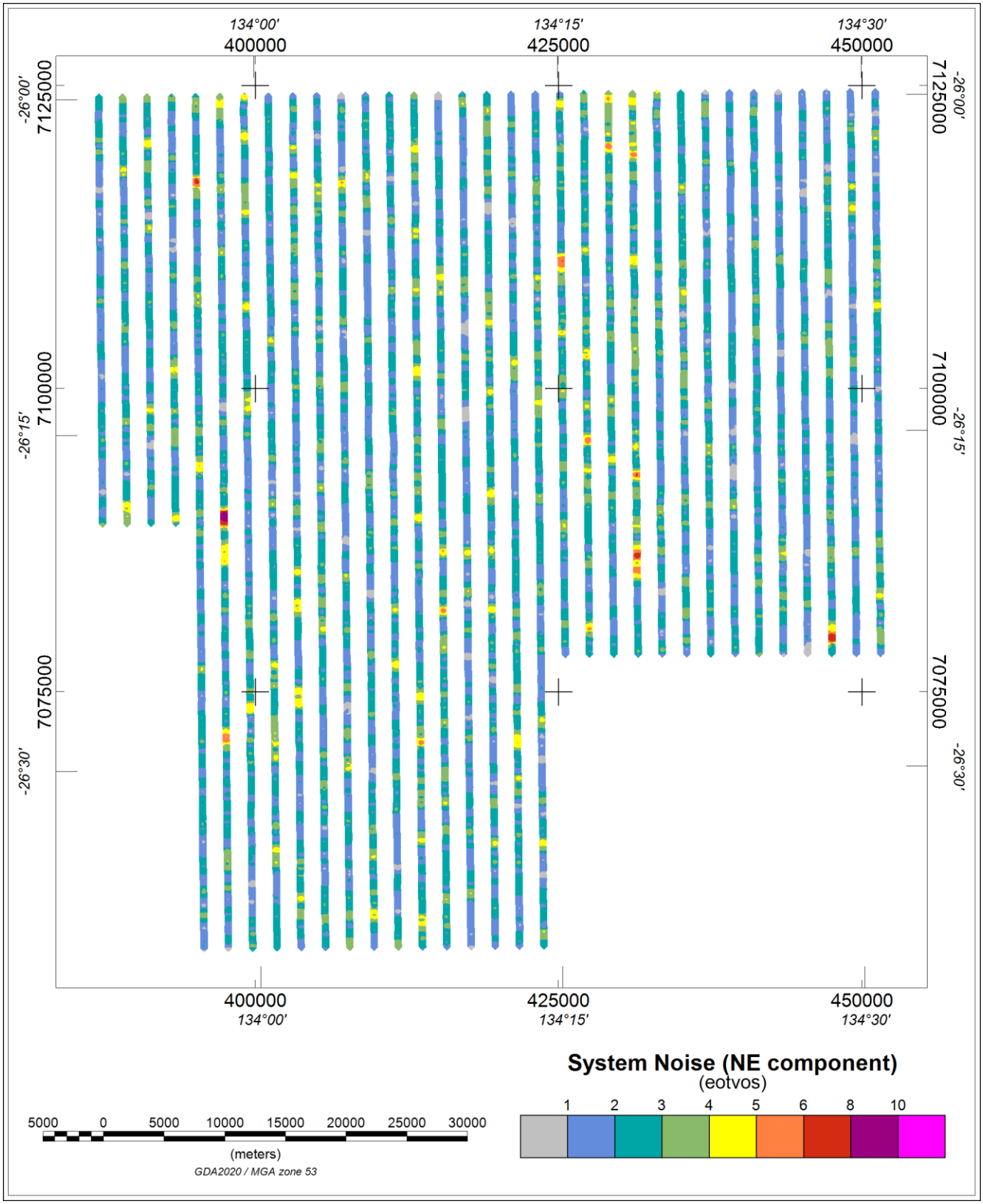

Figure 4: Central Australia Minerals – System Noise NE (eotvos)

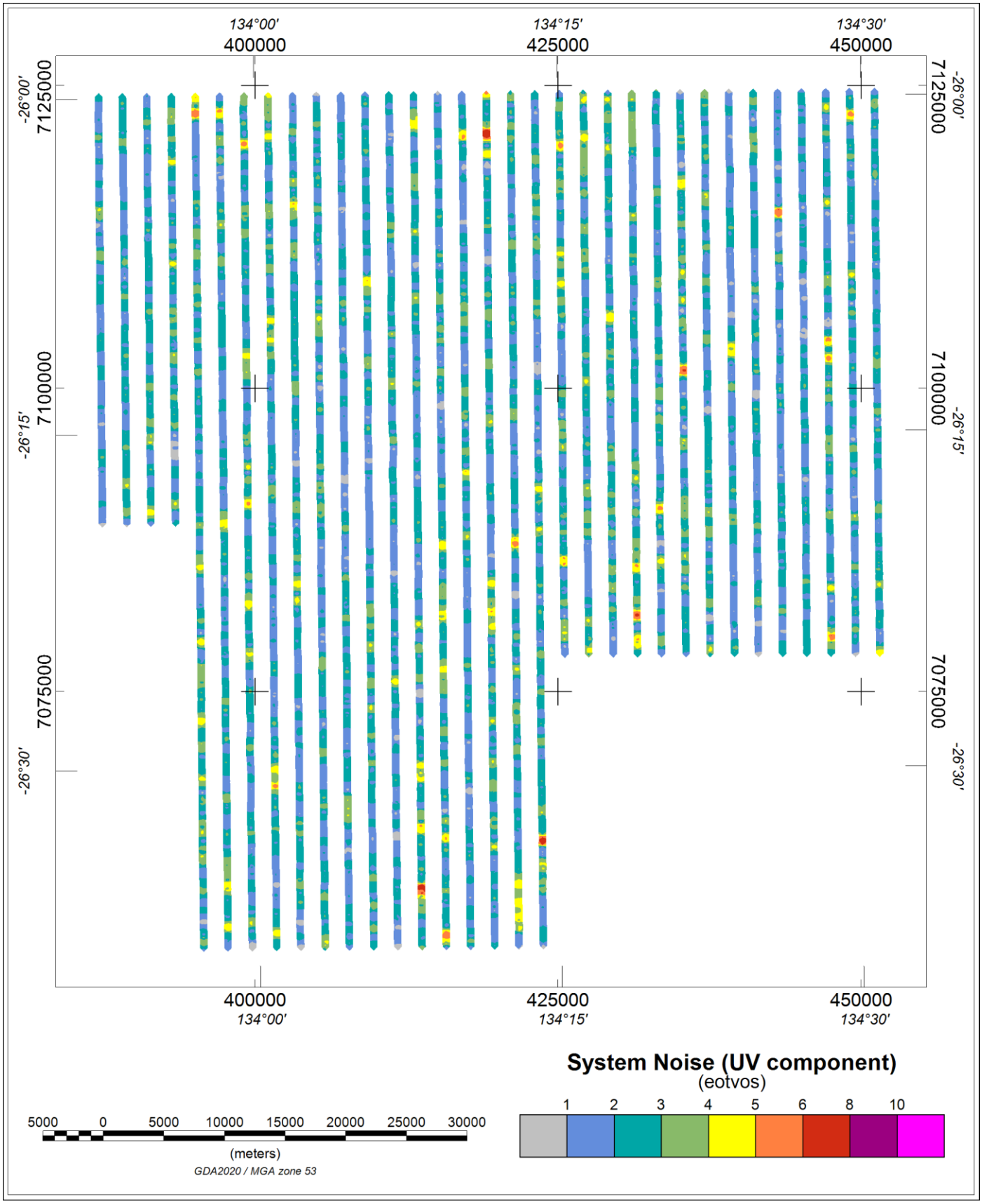

Figure 5: Central Australia Minerals – System Noise UV (eotvos)

4.5 Digital Terrain Model

Laser scanner range data were combined with GPS position and height data (adjusted from height above the WGS84 ellipsoid to height above the geoid by applying the Earth Gravitational Model 1996 (EGM96)). The output of this process is a “swath” of terrain elevations extending either side of the aircraft flight path. Width and sample density of this swath varies with aircraft height. Typical values are 100 to 150 metres and 5 to 10 metres respectively.

Because terrain correction of AGG data requires knowledge of the terrain at distances up to at least 40 km from the data location, laser scanner data collected only along the survey line path must be supplemented by data from another source.

For this purpose, Geoscience Australia DEM-S (one arc second resolution) data are used.

Laser scanner data quality was good with scan density generally above 90%. Laser scanner data were gridded at 20 m with a 1 cell maximum extension beyond data limits. To fill gaps between lines and extend data coverage beyond the survey area, DEM-S grid data were excised to an area 65 km beyond the planned survey area. The excised data were adjusted to the level of the laser scanner data using a grid difference adjustment method. The two grids were then combined into a single grid such that unmodified laser scanner data were used where defined and adjusted DEM-S data were used to fill the gaps and extend the area.

Figure 6 shows the final Digital Terrain Model for the survey area.

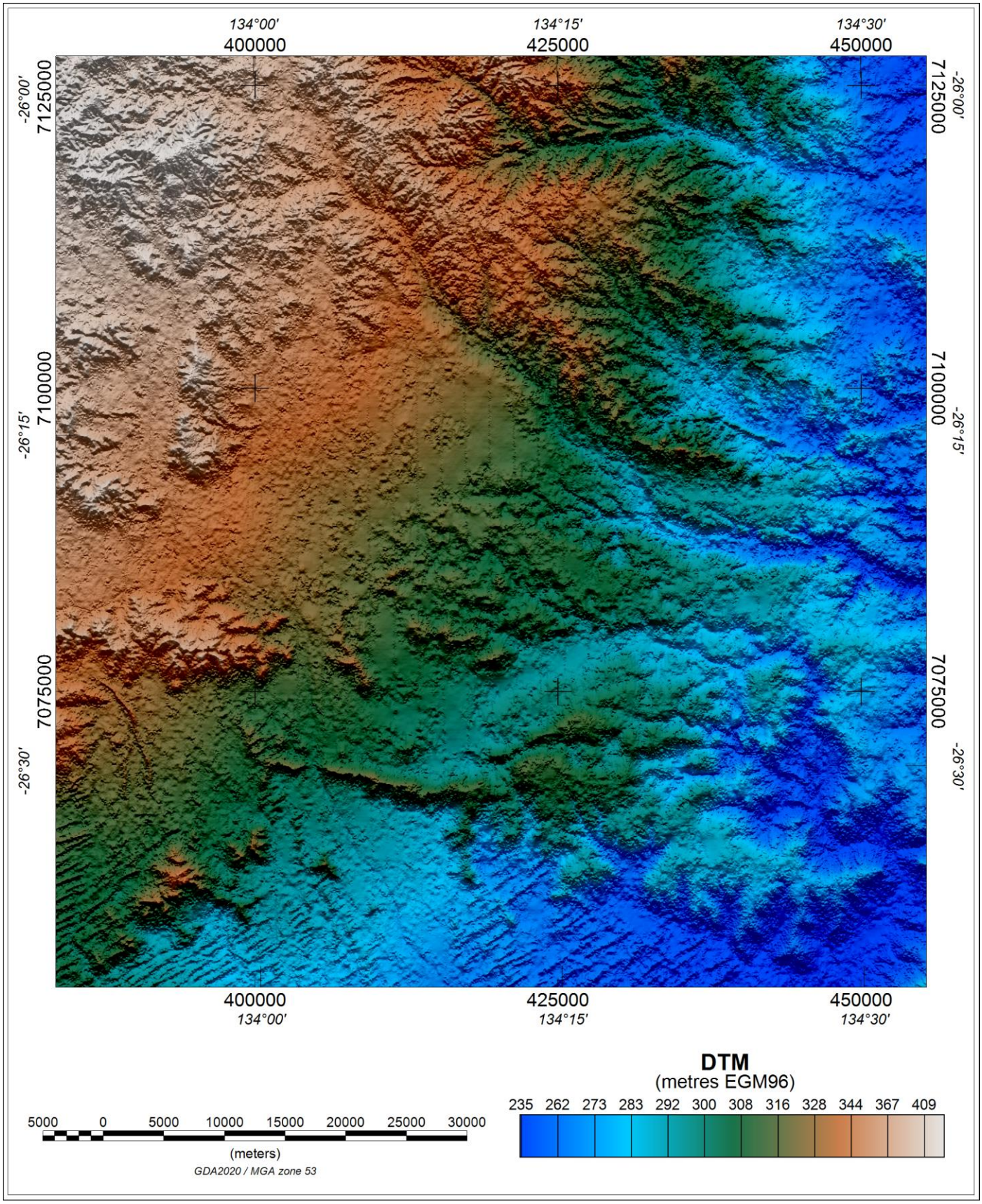

Figure 6: Central Australia Minerals – Final Digital Terrain Model (metres, referenced to the EGM96 geoid)

4.6 Drape Surface Deviation

Flying height for the Central Australia Minerals survey was determined by a pre-computed “drape surface”; designed to create a smooth flight surface, maximising both acquisition quality and safety. The average deviation of actual flying height from this surface was 2.4 m across the survey area. The deviation is shown in *Figure 7.*

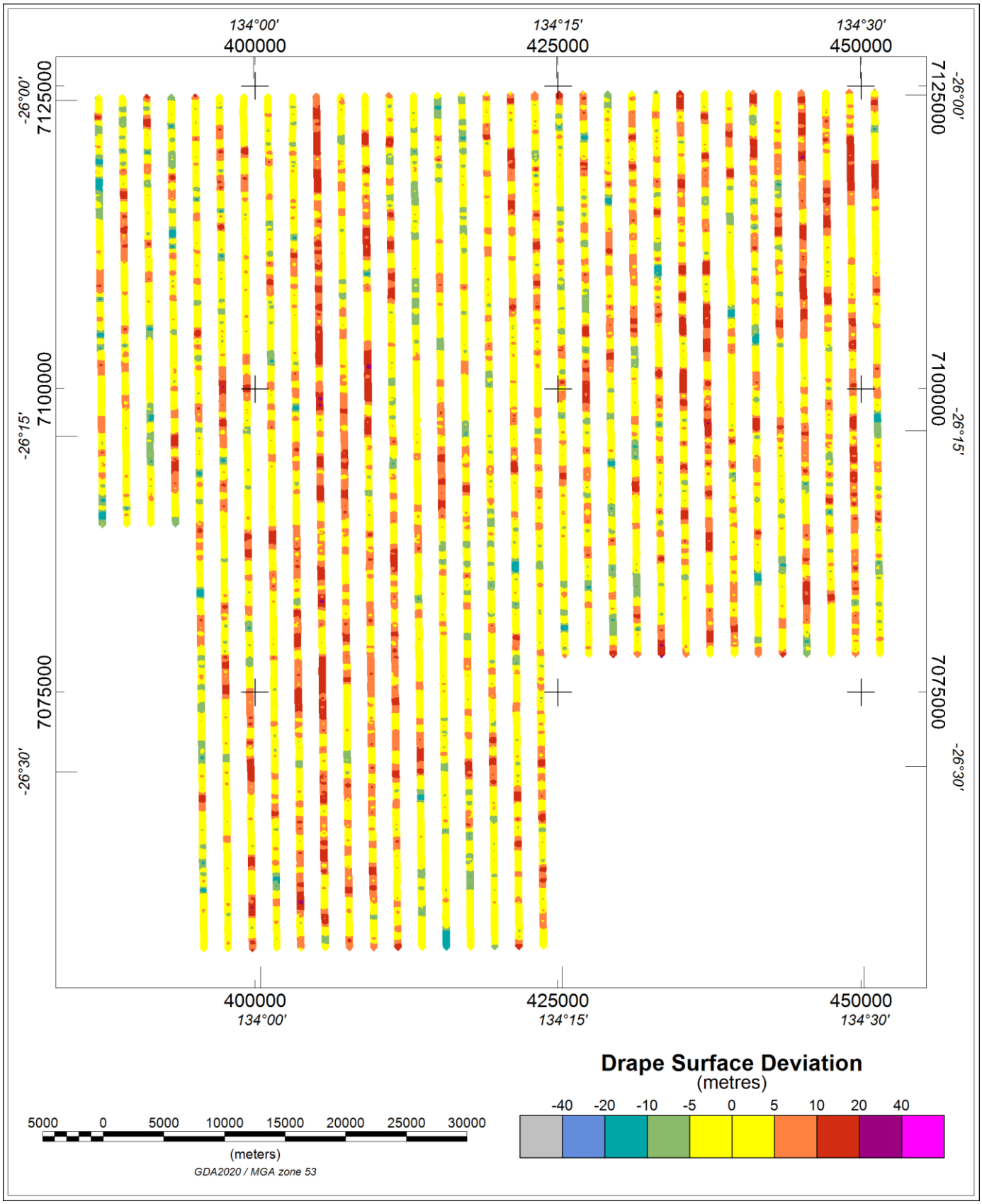

Figure 7: Central Australia Minerals – Deviation from drape surface (metres)

5 FALCON® AIRBORNE GRAVITY GRADIENT (AGG) RESULTS

5.1 Processing Summary

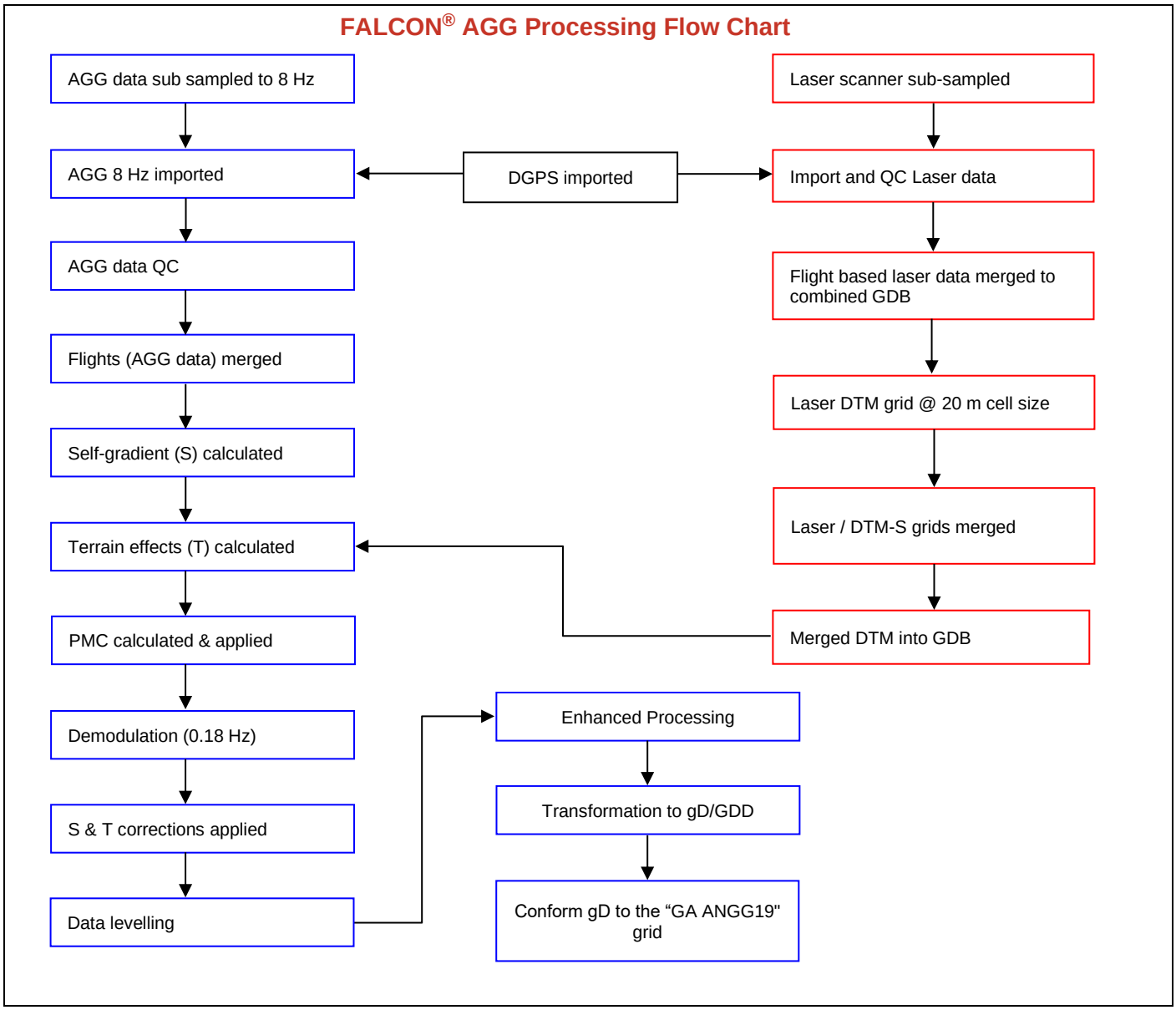

Figure 8: FALCON® AGG Data Processing

5.2 FALCON® Airborne Gravity Gradiometer Data

Figure 8 summarises the steps involved in processing the AGG data obtained from the survey.

The **FALCON®** Airborne Gravity Gradiometer data were digitally recorded by the ADAS on removable hard drives. The raw data were then copied to the field processing laptop, backed up twice onto hard disk media and transferred by Secure File Transfer to the Xcalibur Multiphysics secure server.

Preliminary processing and QC of the **FALCON®** AGG data were completed on-site using Xcalibur Multiphysics' AGG QC software. Further QC and final **FALCON®** AGG data processing were performed by the office-based data processor.

5.3 Radar Altimeter Data

The terrain clearance measured by the radar altimeter in metres was recorded at 10 Hz. The data were plotted and inspected for quality.

5.4 Laser Scanner Data

Laser scanner returns were recorded at a rate of 36 scans per second with each scan returning 276 data points. Each return was converted to ground surface elevation by combining scanner range and angle data with aircraft position and attitude data. Computed elevations were then sub sampled by first dividing each scan into ten segments and combining five adjacent scans per segment, then using a special algorithm to select the optimum return within each data "bin" thus formed. Sub-sampled laser scanner data were edited to remove spikes prior to gridding.

5.5 Positional Data

Differential GPS processing was applied to compute accurate aircraft positions once per second. Waypoint's GrafNav GPS processing software calculated DGPS positions using raw range data obtained from receivers in the aircraft and at a fixed ground base station.

The GPS ground station position was determined by sending several hours of collected data to an online GPS processing service to obtain a differentially corrected computed position. The service selected was AUSPOS, which is provided by Geoscience Australia. The GPS data were processed and quality controlled using the WGS84 datum.

Parameters for the WGS84 datum are:

Ellipsoid: WGS84

Semi-major axis: 6,378,137.0 m

Inverse flattening (1/f): 298.257

All processing was performed using WGS84/UTM Zone 53S coordinates. Final line data and final grid data were supplied in GDA2020/MGA53.

Ellipsoid: GRS80

Semi-major axis: 6,378,137.0 m

Inverse flattening (1/f): 298.257222101

5.6 Terrain Correction

Terrain corrections were derived from the digital terrain model grid for every data point in the survey. A terrain density of 1.00 g/cm^3 was used to compute the terrain correction channels, which were then multiplied by the chosen correction density before being subtracted from the data.

In consultation with the Client, a correction density of 2.1 g/cm^3 was selected as approximating most closely the density of the terrain in the survey area and was applied. As standard, a density of 2.67 g/cm^3 was also applied and these data are also included.

5.7 Regional Levelling

The terrain corrected data and the uncorrected data were then adjusted to the mean regional data (using Geoscience Australia's "2019 Australian National Gravity Grids" (ANGG19)), separately for each line.

5.8 Enhanced Processing

The enhanced processing technique improves the noise amplitude density (as discussed by Christensen et al, 2015) by 25-50% for surveys with line spacing of less than 1 km. The method exploits the different spatial frequencies of system noise and geologic signal. After converting the data into the 2D spatial domain, a custom spatial filter is applied that removes the system noise, while retaining the remaining geologic signal. The process will limit the data resolution to the survey line spacing. The Falcon Difference Noise of the standard product is 2.80 E at 172 m resolution and after applying the processing enhancement, the Falcon Difference Noise is reduced to 1.20 E at 2000 m resolution. Calculating the noise amplitude density is a more appropriate means to evaluate noise with data at different resolutions. The standard product has a noise amplitude density of 1.64 E√km and the enhanced product has a noise amplitude density of 1.60 E√km.

5.9 FALCON® Airborne Gravity Gradient Data - G_{DD} & g_D

The transformation into G_{DD} and g_D was accomplished using a Fourier domain transformation method.

5.9.1 Fourier Transformation

The Fourier domain transformation method firstly calculates many flat surfaces at constant intervals between the lowest and highest-flying altitude. The transformation is performed on each of these surfaces and the result is a three-dimensional array

for each tensor component where each level corresponds to a flat layer of a constant flying height. Using an approximation, the data is interpolated from this array back onto the processing drape surface.

5.9.2 Drape Surface

The transformation uses a smoothed surface onto which the output data are projected. This surface is a smoother equivalent of the actual flying surface.

The Fourier (density 2.1 g/cm^3) G_{DD} map is shown in *Figure 9*.

The Fourier vertical gravity (g_D), derived by integrating $G_{DD,}$ (density 2.1 g/cm^3) result is presented in *Figure 10*.

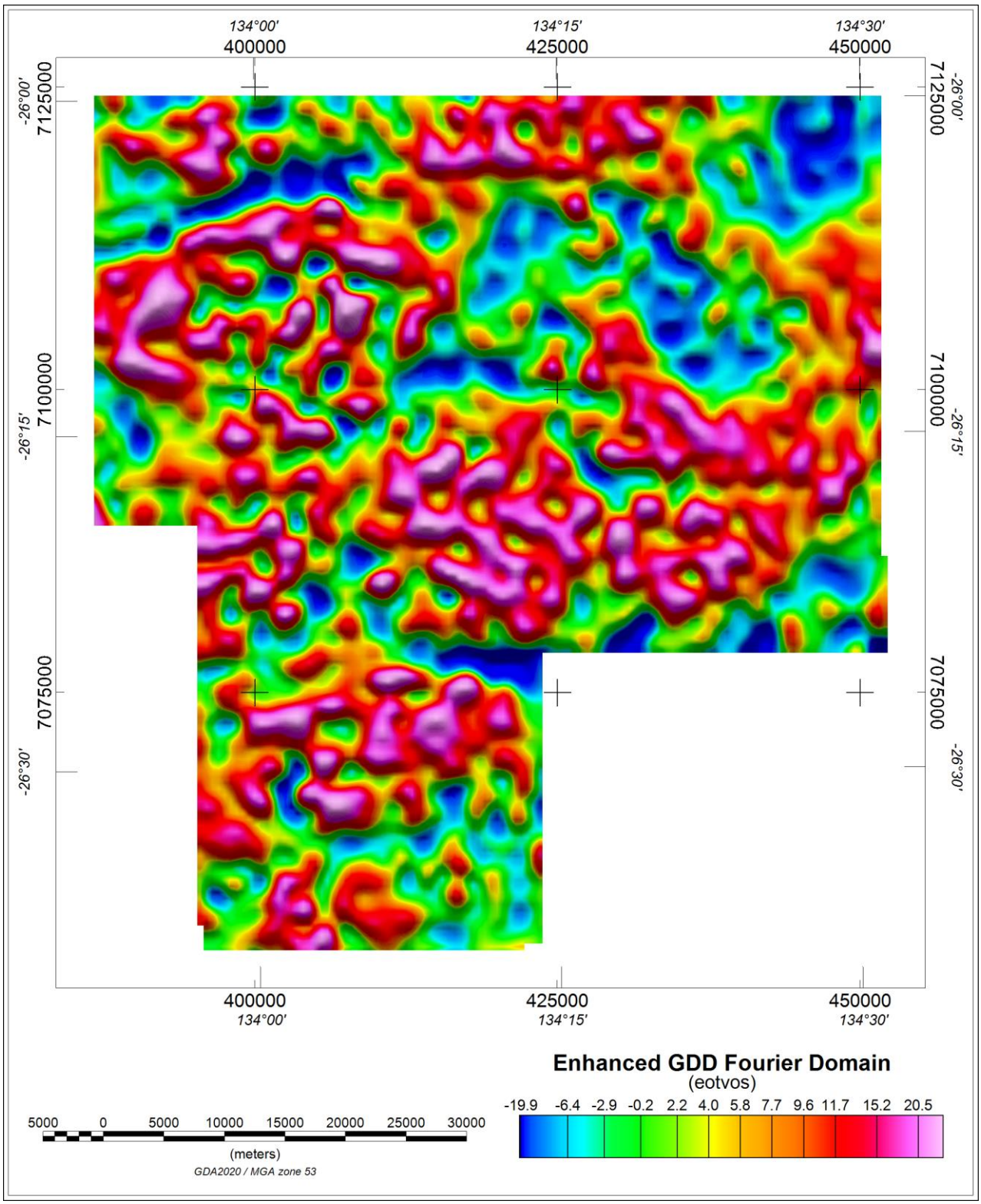

Figure 9: Central Australia Minerals – Enhanced Vertical Gravity Gradient (GDD) from Fourier processing (eotvos).

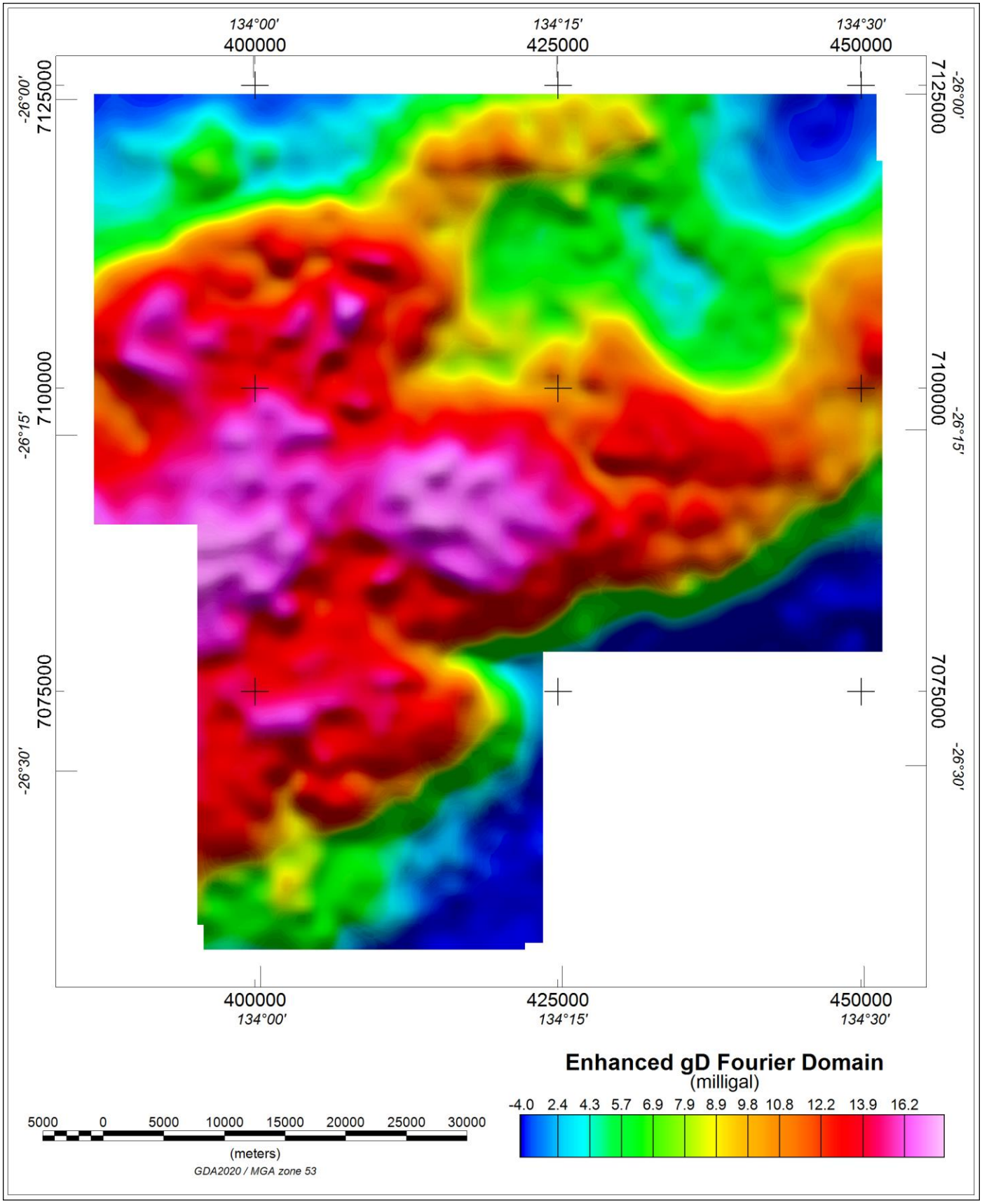

Figure 10: Central Australia Minerals – Enhanced Vertical Gravity (gD) from Fourier processing (milligal)

5.10 Conforming to regional gravity

As discussed in section *8.3*, the long wavelength information in g_D and G_{DD} can be improved by incorporating ancillary information. Such information is available in the form of the Geoscience Australia "2019 Australian National Gravity Grids" (ANGG19).

The g_D and G_{DD} grids were conformed to a subset of the ANGG19 grid as follows. The g_D (density 2.1 g/cm^3) results are presented in *Figure 11*.

- Low pass filter the regional data using a cosine squared filter with cut-off at 30 km, tapering to 20 km.
- High pass filter the g_D and G_{DD} data using a cosine squared filter with cut-off at 30 km, tapering to 20 km.
- Conform the g_D and G_{DD} data to the regional data by addition of the filtered grids. The filter design is such that this method provides uniform frequency response across the overlap frequencies.

Further discussion of this method can be found in Dransfield (2010).

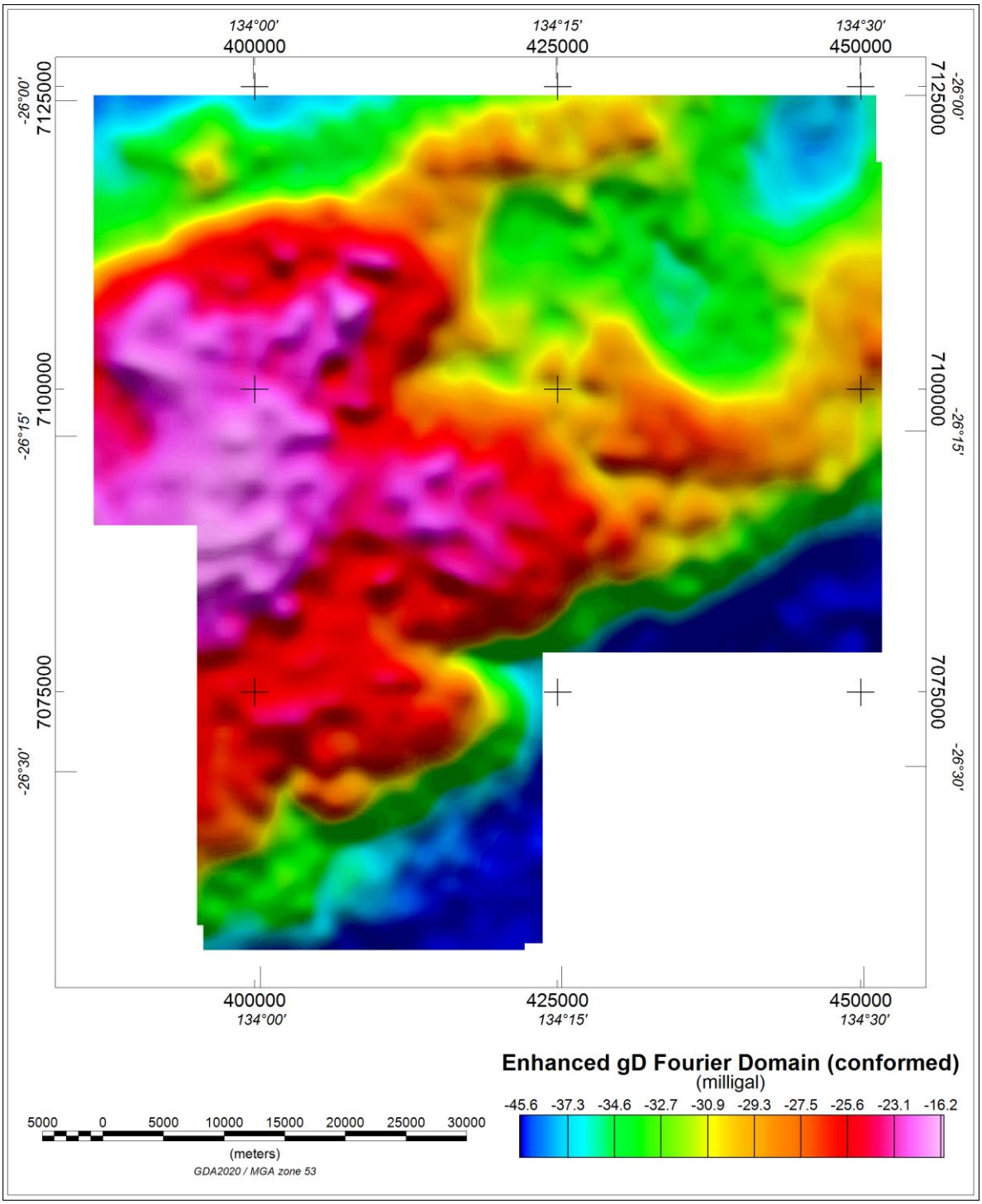

Figure 11: Central Australia Minerals – Enhanced Vertical Gravity (gD) from Fourier processing conformed to regional gravity data (milligal)

6 APPENDIX I - SURVEY EQUIPMENT

6.1 Survey Aircraft

An Xcalibur Multiphysics Cessna C208B turbo prop, Australian registration VH-HFX was used to fly the survey area. The following instrumentation was used for this survey.

6.2 FALCON® Airborne Gravity Gradiometer

FALCON® AGG System (Newton)

The **FALCON®** AGG System is based on current state-of-the-art airborne gravity gradiometer technology and has been optimized for airborne broadband geophysical exploration. The system is capable of supporting surveying activities in areas ranging from 1,000 ft below sea level to 13,000 ft above sea level with aircraft speeds from 30 to 130 knots. The FALCON® AGG data streams were digitally recorded at different rates on removable drives installed in the FALCON® AGG electronics rack.

6.3 Airborne Data Acquisition Systems

Digital Acquisition System (FASDAS)

The FASDAS is a data acquisition system executing propriety software for the acquisition and recording of location, magnetic and ancillary data. Data are presented both numerically and graphically in real time on the VGA display providing on-line quality control capability.

The FASDAS is also used for real time navigation. A pre-programmed flight plan, containing boundary coordinates, line start and end coordinates, altitude values calculated for a theoretical drape surface, line spacing and cross track definitions is loaded into the computer prior to each flight. The WGS84 latitude, longitude and altitude received from the real-time corrected, dual frequency Novatel positioning receiver, is transformed to the local coordinate system for cross track and distance to go values. This information, together with ground heading and speed, is displayed to the pilot numerically and graphically on a two-line LCD display. It is also presented on the operator LCD screen in conjunction with a pictorial representation of the survey area, survey lines and ongoing flight path.

FALCON® AGG Data Acquisition System (ADAS)

The ADAS provides control and data display for the FALCON® AGG system. Data are displayed in real time for the operator and warnings displayed should system parameters deviate from tolerance specifications. All FALCON® AGG and laser scanner data are recorded to a removable hard drive.

6.4 Real-Time Differential GPS

The **Novatel OEMV-3-L1L2** multi-frequency positioning receiver provides real-time differential GNSS for the on-board navigation system. The OEMV-3 is designed to track the GPS L1 and L2 signals, as well as GLONASS L1 and L2. The differential data set is relayed via a geo-synchronous satellite to the aircraft where the receiver optimized the corrections for the current location.

6.5 GPS Base Station Receiver

The **Javad Triumph-1** is a 216-channel, multi-frequency GNSS receiver. It can provide raw range information of all satellites in view from the GPS, GLONASS, BeiDou and Galileo satellite systems. The receiver can sample at up to 5 Hz and records to internal memory. These data are used to provide post-processed differential GNSS (DGNSS) corrections for the rover data flight path.

6.6 Altimeter

King KRA405B Radar Altimeter

The radar altimeter has an accuracy of 3 ft or ±3% at 0-500 ft and ±5% at 500-2500 ft, a range of 0-2,500 ft and a measurement rate of 10 Hz.

6.7 Laser Scanner

Riegl LMS-Q240I-60

The laser scanner is designed for high-speed line scanning applications. The system is based upon the principle of time-of-flight measurement of short laser pulses in the infrared wavelength region and the angular deflection of the laser beam is obtained by a rotating polygon mirror wheel. The measurement range is up to 650 m with a minimum range of 2 m and an accuracy of 20 mm. The laser beam is eye-safe, the laser wavelength is 0.9 μm, the scan angle range is ± 40° and the scan speed is 36 scans/s.

6.8 Data Processing Hardware and Software

The following equipment and software were used:

Hardware

- One 2.0 GHz (or higher) laptop computer
- External USB hard drive reader for ADAS removable drives
- Two External USB hard drives for data backup

Software

- Oasis Montaj data processing and imaging software
- GrafNav Differential GPS processing software
- Xcalibur Multiphysics' Atlas data processing software
- Xcalibur Multiphysics' DiAGG processing software

7 APPENDIX II - SYSTEM TESTS

7.1 Instrumentation Lag

Due to the relative position of the magnetometer, altimeters and GPS antenna on the aircraft and to processing/recording time lags, raw readings from each data stream vary in position. To correct for this and to align selected anomaly features on lines flown in opposite directions, the magnetic and altimeter data are 'parallaxed' with respect to the position information. The lags were applied to the data during processing.

7.2 Radar Altimeter Calibration

The radar altimeter is checked for accuracy and linearity every 12 months, or when any change in a key system component requires this procedure to be carried out. This calibration allows the radar altimeter data to be compared and assessed with the other height data (GPS and laser) to confirm the accuracy of the radar altimeter over its operating range. The calibration is performed by flying a number of 30-second lines at preselected terrain clearances over an area of flat terrain and using the results of the radar altimeter, differentially corrected GPS heights in mean sea level (MSL) and laser scanner were used to derive slope and offset information.

7.3 FALCON® AGG Noise Measurement

At the commencement of the survey, 20 minutes of data were collected with the aircraft in straight level flight at 3500 ft AGL. These data were assessed in-flight to check the AGG noise levels.

Daily flight debriefs incorporating **FALCON®** AGG performance statistics for each flight line are prepared using output from Xcalibur Multiphysics' DiAGG software. These are sent daily to Xcalibur Multiphysics' office staff for performance evaluation.

7.4 Daily Calibrations and checks

A set of daily calibrations and checks were performed each survey day as follows:

7.4.1 FALCON® AGG Quiescent Noise Check

Prior to each day's survey, the AGG quiescent noise levels were checked to verify the system was performing as expected.

7.4.2 FALCON® AGG Calibration

A calibration was performed at the beginning of each flight and the results monitored by the operator. The coefficients obtained from each of the calibrations were used in the processing of the data.

8 APPENDIX III - FALCON® AGG DATA & PROCESSING

8.1 Nomenclature

The **FALCON®** airborne gravity gradiometer (AGG) system adopts a North, East, and Down coordinate sign convention and these directions (N, E, and D) are used as subscripts to identify the gravity gradient tensor components (gravity vector derivatives). Lower case is used to identify the components of the gravity field and upper case to identify the gravity gradient tensor components. Thus, the parameter usually measured in a normal exploration ground gravity survey is $\mathbf{g_D}$ and the vertical gradient of this component is $\mathbf{G_{DD}}$.

8.2 Units

The vertical component of gravity ($\mathbf{g_D}$) is delivered in the usual units of mGal. The gradient tensor components are delivered in eotvos, which is usually abbreviated to "E". By definition **1 E = 10^{-4} mGal/m.**

8.3 FALCON® Airborne Gravity Gradiometer Surveys

In standard ground gravity surveys, the component measured is "$\mathbf{g_D}$", which is the *vertical component of the acceleration due to gravity*. In airborne gravity systems, since the aircraft is itself accelerating, measurement of "$\mathbf{g_D}$" cannot be made to the same precision and accuracy as on the ground. Airborne gravity gradiometry uses a differential measurement to remove the aircraft motion effects and delivers gravity data of a spatial resolution and sensitivity comparable with ground gravity data.

The **FALCON®** gradiometer instrument acquires two curvature components of the gravity gradient tensor namely $\mathbf{G_{NE}}$ and $\mathbf{G_{UV}}$ where $\mathbf{G_{UV}} = (\mathbf{G_{NN}} - \mathbf{G_{EE}})/2$.

A feature of the **FALCON®** AGG system is that two independent measurements are made of both the NE and UV curvature components. This is achieved by using two sets of accelerometers, referred to as the A complement and the B complement. Each complement consists of four accelerometers. The measured gradients from these complements are referred to as A_{NE} and A_{UV} and B_{NE} and B_{UV}. The $\mathbf{G_{NE}}$ and $\mathbf{G_{UV}}$ gradients are computed by averaging A and B:

$$\boldsymbol{G_{NE}} = \frac{(A_{NE} + B_{NE})}{2}$$

$$\boldsymbol{G_{UV}} = \frac{(A_{UV} + B_{UV})}{2}$$

Since these curvature components cannot easily and intuitively be related to the causative geology, they are transformed into the vertical gravity gradient ($\mathbf{G_{DD}}$), and integrated to derive the vertical component of gravity ($\mathbf{g_D}$). Interpreters display, interpret and model both $\mathbf{G_{DD}}$ and $\mathbf{g_D}$. The directly measured $\mathbf{G_{NE}}$ and $\mathbf{G_{UV}}$ data are appropriate for use in inversion software to generate density models of the earth. The vertical gravity gradient, $\mathbf{G_{DD}}$, is more sensitive to small or shallow sources and has greater spatial resolution than $\mathbf{g_D}$ (similar to the way that the vertical magnetic gradient provides greater spatial resolution and increased sensitivity to shallow sources of the magnetic field). In the integration of $\mathbf{G_{DD}}$ to give $\mathbf{g_D}$, the very long wavelength component, at wavelengths comparable to or greater than the size of the survey area, cannot be fully recovered. Long wavelength gravity data are therefore incorporated in the $\mathbf{g_D}$ data from other sources. This might be regional ground, airborne or marine gravity if such data are available. The Danish Technical University global gravity data of 2017 (DTU17) are used as a default if other data are not available.

8.4 Gravity Data Processing

The main elements and sequence of processing of the gravity data are given below. Unless not applicable or specified otherwise, the processing step is applied to each individual complement element (A_{NE}, A_{UV}, B_{NE}, B_{UV}):

1. Dynamic corrections for residual aircraft motion (called Post Mission Compensation or PMC) are calculated and applied.
2. Self-gradient corrections are calculated and applied to reduce the time-varying gradient response from the aircraft and platform.
3. A Digital Terrain Model (DTM) is created from the laser scanner range data, the AGG inertial navigation system rotation data and the DGPS position data.
4. Terrain corrections are calculated and applied.
5. Line levelling and micro-levelling (where necessary) are applied.
6. $\mathbf{G_{NE}}$ and $\mathbf{G_{UV}}$ are transformed into the full gravity gradient tensor, including $\mathbf{G_{DD}}$, and into $\mathbf{g_D}$.

8.5 Aircraft Dynamic Corrections

The design and operation of the **FALCON®** AGG results in very considerable reduction of the effects of aircraft acceleration but residual levels are still significant and further reduction is required and must be done in post-processing.

Post-processing correction relies on monitoring the inertial acceleration environment of the gravity gradiometer instrument (GGI) and constructing a model of the response of the GGI to this environment. Parameters of the model are adjusted by regression to match the sensitivity of the GGI during data acquisition. The modelled GGI output in response to the inertial sensitivities is subtracted from the observed output. Application of this technique to the output of the GGI, when it is adequately compensated by its internal mechanisms, reduces the effect of aircraft motion to acceptable levels.

Following these corrections, the gradient data are demodulated and filtered along line using a 6-pole Butterworth low-pass filter with a cut-off frequency of 0.18 Hz.

8.6 Self-gradient Corrections

The GGI is mounted in gimbals controlled by an inertial navigation system, which keeps the GGI pointing in a fixed direction whilst the aircraft and gimbals rotate around it. Consequently, the GGI measures a time-varying gravity gradient due to these masses moving around it as the heading and attitude of the aircraft changes during flight. This is called the self-gradient.

Like the aircraft dynamic corrections, the self-gradient is calculated by regression of model parameters against measured data. In this case, the rotations of the gimbals are the input variables of the model. Once calculated, the modelled output is subtracted from the observed output.

8.7 Laser Scanner Processing

The laser scanner measures the range from the aircraft to the ground in a swath of angular width ±40 degrees below the aircraft. The aircraft attitude (roll, pitch and heading) data provided by the AGG inertial navigation system are used to adjust the range data for changes in attitude and the processed differential GPS data are used to reference the range data to located ground elevations referenced to the WGS84 datum (corrected for the EGM96 geoid separation model). Statistical filtering strategies are used to remove anomalous elevations due to foliage or built-up environment. The resulting elevations are gridded to form a digital terrain model (DTM).

8.8 Terrain Corrections

An observation point above a hill has excess mass beneath it compared to an observation point above a valley. Since gravity is directly proportional to the product of the masses, uncorrected gravity data have a high correlation with topography.

It is therefore necessary to apply a terrain correction to gravity survey data. For airborne gravity gradiometry at low survey heights, a detailed DTM is required. Typically, immediately below the aircraft, the digital terrain will need to be sampled at a cell size roughly one-third to one-half of the survey height and with a position accuracy of better than 1 metre. For these accuracies, LIDAR data are required and each **FALCON®** survey aircraft comes equipped with LIDAR (laser scanner).

If bathymetric data are used, then these form a separate terrain model for which terrain corrections are calculated at a density chosen to suit the water bottom – water interface.

Once the DTM has been merged, the terrain corrections for each of the $\mathbf{G_{NE}}$ and $\mathbf{G_{UV}}$ data streams are calculated. In the calculation of terrain corrections, a density of 1 g/cm^3 is used. The calculated corrections are stored in the database allowing the use of any desired terrain correction density by subtracting the product of desired density and correction from the measured $\mathbf{G_{NE}}$ and $\mathbf{G_{UV}}$ data. The terrain correction density is chosen to be representative of the terrain density over the survey area. Sometimes more than one density is used with input from the Client.

Typically, the terrain corrections are calculated over a distance 40 to 60 km from each survey measurement point.

8.9 Regional Levelling

The terrain and self-gradient corrected $\mathbf{G_{NE}}$ and $\mathbf{G_{UV}}$ data are adjusted to the regional data, separately for each line. Occasionally some micro-levelling might be performed.

8.10 Transformation into GDD & g_D

The transformation of the measured, corrected and levelled $\mathbf{G_{NE}}$ and $\mathbf{G_{UV}}$ data into gravity and components of the full gravity gradient tensor is accomplished using a Fourier domain transformation method.

The input data for the Fourier method are the average **NE** and **UV** components computed from the complement data, as described in section *8.3*. The Fourier method relies on the Fourier transform of Laplace's equation. The application of this transform to the complex function $\mathbf{G_{NE} + i\, G_{UV}}$ provides a stable and accurate calculation of each of the full tensor components and gravity. The Fourier method performs piece-wise upward and downward continuation to work with data collected on a surface that varies from a flat horizontal plane. For stability of the downward continuation, the data are low-

pass filtered. The cut-off wavelength of this filter depends on the variations in altitude range and line spacing. It is set to the smallest value that provides stable downward continuation.

The limitations of gravity gradiometry in reconstructing the long wavelengths of gravity can lead to uncertainties in the longer wavelength values. The merging of the $\mathbf{g_D}$ data with externally supplied regional gravity such as the DTU17 gravity provides a way of reducing these uncertainties. The application of this procedure will depend on the survey size and resolution of available regional gravity. If survey size is too small or regional gravity resolution too large, regional conforming is not applied.

8.11 Terrain Corrections Using Alternate Terrain Densities

Although both uncorrected processed and transformed data and unit density terrain correction data are supplied, it is not recommended that these be used to create final data corrected for any arbitrary terrain correction density. The principal reason for this is that tie line levelling occurs after application of the terrain correction. As a result, levelling errors present in the terrain correction channels by virtue of positional inaccuracy are not removed from these channels and will be present in any data corrected with them. Further, filtering applied in creating the uncorrected, transformed data is not applied to the terrain correction channels. Mixing data filtered in different ways is not advised.

An alternative method (valid only for datasets where waterbody(ies) have not been taken into account when computing the terrain corrections) uses the linear relationship between the terrain corrections at different densities and the corresponding gravity gradient or $\mathbf{g_D}$ values. This method can be applied to either the grid data or the located data. An example is given using $\mathbf{G_{DD}}$:

The new density is referred to as ρ_N, the existing densities as ρ_1 and ρ_2

$$G_{DD}(\rho_N) = G_{DD}(\rho_1) + \left(G_{DD}(\rho_2) - G_{DD}(\rho_1)\right) \times \frac{(\rho_N - \rho_1)}{(\rho_2 - \rho_1)}$$

Note that the terrain correction channel is eliminated by substitution in deriving this equation.

It is recommended that two densities that differ by a reasonable value be used for this method, in order to minimise uncertainties caused by noise in the data. The values of 0.00 and 2.67 g/cm^3 usually delivered should be sufficient to yield useful results.

8.12 Noise & Signal

By taking two independent measurements of the NE and UV curvature components at each sample point, it is possible to obtain a direct indication of the reliability of these measurements. The standard deviation of half the difference of the pairs of measurements - (A_{NE},B_{NE}) and (A_{UV},B_{UV}) - provides a good estimate of the survey noise:

$$Noise_{NE} = StdDev\left(\frac{(A_{NE} - B_{NE})}{2}\right)$$

$$Noise_{UV} = StdDev\left(\frac{(A_{UV} - B_{UV})}{2}\right)$$

These difference channels are calculated for each data point. The standard deviation across all data points is the figure quoted for the survey as a whole.

This difference error has been demonstrated to follow a ‘normal’ or Gaussian statistical distribution, with a mean of zero. Therefore, the bulk of the population (95%) will lie between -2σ and +2σ of the mean. For a typical survey noise estimate of, say, 3 E, 95% of the noise will be between -6 E and +6 E.

These typical errors in the curvature gradients translate to errors in $\mathbf{G_{DD}}$ of about 5 E and in $\mathbf{g_D}$ (in the shorter wavelengths) in the order of 0.1 mGal.

8.13 Risk Criteria in Interpretation

The risks associated with a **FALCON®** AGG survey are mainly controlled by the following factors.

- **Survey edge anomalies** – the transformation from measured curvature gradients to vertical gradient and vertical gravity gradient is subject to edge effects. Hence, any anomalies located within about 2 x line spacing of the edge of the survey boundaries should be treated with caution.
- **Single line anomalies** – for a wide-spaced survey, an anomaly may be present on only one line. Although it might be a genuine anomaly, the interpreter should note that no two-dimensional control can be applied.
- **Low amplitude (less than 2σ) anomalies** – Are within the noise envelope and need to be treated with caution if they are single line anomalies and close in diameter to the cut-off wavelengths used.

- **Residual topographic error anomalies** – Inaccurate topographic correction either due to inaccurate DTM or local terrain density variations may produce anomalies. Comparing the DTM with the G_{DD} map terrain-corrected for different densities is a reliable way to confirm the legitimacy of an anomaly.
- **The low density of water and lake sediments** – (if present) can create significant gravity and gravity gradient lows, which may be unrelated to bedrock geology. It is recommended that all anomalies located within lakes or under water be treated with caution and assessed with bathymetry if available.

8.14 References

Boggs, D. B. and Dransfield, M. H., 2004, Analysis of errors in gravity derived from the Falcon® airborne gravity gradiometer, Lane, R. (ed.), Airborne Gravity 2004 - Abstracts from the ASEG-PESA Airborne Gravity 2004 Workshop, Geoscience Australia Record 2004/18, 135-141.

Christensen A.N., Dransfield, M. H. and Van Galder C, 2015, Noise and repeatability of airborne gravity gradiometry, First Break, Volume 33, April 2015, 55 - 63.

Dransfield, M. H., 2010, Conforming Falcon gravity and the global gravity anomaly, Geophysical Prospecting, 58, 469-483.

Dransfield, M. H. and Lee, J. B., 2004, The FALCON® airborne gravity gradiometer survey systems, Lane, R. (ed.), Airborne Gravity 2004 - Abstracts from the ASEG-PESA Airborne Gravity 2004 Workshop, Geoscience Australia Record 2004/18, 15-19.

Dransfield, M. H. and Zeng, Y., Airborne gravity gradiometry: terrain corrections and elevation error, Geophysics 2009/Sep 74(5).

Lee, J. B., 2001, FALCON Gravity Gradiometer Technology, Exploration Geophysics, 32, 75-79.

Lee, J. B.; Liu, G.; Rose, M.; Dransfield, M.; Mahanta, A.; Christensen, A. and Stone, P., 2001, High resolution gravity surveys from a fixed wing aircraft, Geoscience and Remote Sensing Symposium, 2001. IGARSS '01. IEEE 2001 International, 3, 1327-1331.

Stone, P. M. and Simsky, A., 2001, Constructing high resolution DEMs from Airborne Laser Scanner Data, Preview, Extended Abstracts: ASEG 15th Geophysical Conference and Exhibition, August 2001, Brisbane, 93, 99.

9 APPENDIX IV - FINAL PRODUCTS

Final **FALCON®** AGG digital line data were provided in an 8 Hz ASCII database file containing the fields and format described in *Table 5* below.

Grids of AGG products, as well as the DTM were delivered, as described in *Table 6* below. The grids are in ERMapper ERS format with a 500 m cell size, with the exception of the DTM grids which have a 20 m cell size.

One copy of the digital archives was delivered along with a copy of this Logistics and Processing Report.

Field	Variable	Description	Units
1	Line	Line number	
2	Flight	Flight number	
3	Date	Gregorian date	YYYYMMDD
4	Time	Universal Time (seconds since January 6 1980)	seconds
5	Easting	GDA2020/MGA53 Easting	metres
6	Northing	GDA2020/MGA53 Northing	metres
7	Longitude	GDA2020 longitude	degrees
8	Latitude	GDA2020 latitude	degrees
9	Altitude_Ellipsoid	GPS antenna height above GDA2020 ellipsoid	metres
10	Altitude	GPS antenna height above sea level (referenced to EGM96 geoid)	metres
11	DTM	Terrain height above sea level (referenced to EGM96 geoid) (sampled from final DTM grid)	metres
12	Height	Flying height (aircraft's height above terrain as derived from DTM and ALTITUDE channels)	metres
13	Turbulence	Estimated vertical platform turbulence (vertical acceleration where g = 9.80665 m/sec/sec)	milli g
14	T_DD	Terrain effect calculated for DD using a density of 1 g/cc (from final DTM grid)	eotvos
15	T_NE	Terrain effect calculated for NE using a density of 1 g/cc (from final DTM grid)	eotvos
16	T_UV	Terrain effect calculated for UV using a density of 1 g/cc (from final DTM grid)	eotvos
17	Err_NE	NE gradient uncorrelated noise estimate after levelling	eotvos
18	Err_UV	UV gradient uncorrelated noise estimate after levelling	eotvos
19	A_NE_2p67	Self gradient & terrain corrected NE gradient using terrain correction density 2.67 g/cc	eotvos
20	A_UV_2p67	Self gradient & terrain corrected UV gradient using terrain correction density 2.67 g/cc	eotvos
21	B_NE_2p67	Self gradient & terrain corrected NE gradient using terrain correction density 2.67 g/cc	eotvos
22	B_UV_2p67	Self gradient & terrain corrected UV gradient using terrain correction density 2.67 g/cc	eotvos
23	A_NE_2p1	Self gradient & terrain corrected NE gradient using terrain correction density 2.1 g/cc	eotvos
24	A_UV_2p1	Self gradient & terrain corrected UV gradient using terrain correction density 2.1 g/cc	eotvos
25	B_NE_2p1	Self gradient & terrain corrected NE gradient using terrain correction density 2.1 g/cc	eotvos

26	B_UV_2p1	Self gradient & terrain corrected UV gradient using terrain correction density 2.1 g/cc	eotvos
27	A_NE_0	Self gradient corrected NE gradient only with no terrain correction applied	eotvos
28	A_UV_0	Self gradient corrected UV gradient only with no terrain correction applied	eotvos
29	B_NE_0	Self gradient corrected NE gradient only with no terrain correction applied	eotvos
30	B_UV_0	Self gradient corrected UV gradient only with no terrain correction applied	eotvos
31	gD_Fourier_2p67	Enhanced Fourier derived vertical Gravity using terrain correction density 2.67 g/cc	mGal
32	gD_Fourier_2p67_conformed	Regional conformed enhanced Fourier derived vertical Gravity using terrain correction density 2.67 g/cc	mGal
33	GDD_Fourier_2p67	Enhanced Fourier derived vertical gravity gradient using terrain correction density 2.67 g/cc	eotvos
34	GDD_Fourier_2p67_conformed	Regional conformed enhanced Fourier derived vertical gravity gradient using terrain correction density 2.67 g/cc	eotvos
35	GEE_Fourier_2p67	Enhanced Fourier derived Gee gravity gradient using terrain correction density 2.67 g/cc	eotvos
36	GNN_Fourier_2p67	Enhanced Fourier derived Gnn gravity gradient using terrain correction density 2.67 g/cc	eotvos
37	GED_Fourier_2p67	Enhanced Fourier derived Ged horizontal EW gravity gradient using terrain correction density 2.67 g/cc	eotvos
38	GND_Fourier_2p67	Enhanced Fourier derived Gnd horizontal NS gravity gradient using terrain correction density 2.67 g/cc	eotvos
39	GNE_Fourier_2p67	Enhanced Fourier derived Gne gravity curvature gradient using terrain correction density 2.67 g/cc	eotvos
40	GUV_Fourier_2p67	Enhanced Fourier derived Guv gravity curvature gradient using terrain correction density 2.67 g/cc	eotvos
41	gD_Fourier_2p1	Enhanced Fourier derived vertical Gravity using terrain correction density 2.1 g/cc	mGal
42	gD_Fourier_2p1_conformed	Regional conformed enhanced Fourier derived vertical Gravity using terrain correction density 2.1 g/cc	mGal
43	GDD_Fourier_2p1	Enhanced Fourier derived vertical gravity gradient using terrain correction density 2.1 g/cc	eotvos
44	GDD_Fourier_2p1_conformed	Regional conformed enhanced Fourier derived vertical gravity gradient using terrain correction density 2.1 g/cc	eotvos
45	GEE_Fourier_2p1	Enhanced Fourier derived Gee gravity gradient using terrain correction density 2.1 g/cc	eotvos
46	GNN_Fourier_2p1	Enhanced Fourier derived Gnn gravity gradient using terrain correction density 2.1 g/cc	eotvos
47	GED_Fourier_2p1	Enhanced Fourier derived Ged horizontal EW gravity gradient using terrain correction density 2.1 g/cc	eotvos
48	GND_Fourier_2p1	Enhanced Fourier derived Gnd horizontal NS gravity gradient using terrain correction density 2.1 g/cc	eotvos
49	GNE_Fourier_2p1	Enhanced Fourier derived Gne gravity curvature gradient using terrain correction density 2.1 g/cc	eotvos
50	GUV_Fourier_2p1	Enhanced Fourier derived Guv gravity curvature gradient using terrain correction density 2.1 g/cc	eotvos

51	gD_Fourier_0	Enhanced Fourier derived vertical Gravity with no terrain correction applied	mGal
52	gD_Fourier_0_conformed	Regional conformed enhanced Fourier derived vertical Gravity with no terrain correction applied	mGal
53	GDD_Fourier_0	Enhanced Fourier derived vertical gravity gradient with no terrain correction applied	eotvos
54	GDD_Fourier_0_conformed	Regional conformed enhanced Fourier derived vertical gravity gradient with no terrain correction applied	eotvos
55	GEE_Fourier_0	Enhanced Fourier derived Gee gravity gradient with no terrain correction applied	eotvos
56	GNN_Fourier_0	Enhanced Fourier derived Gnn gravity gradient with no terrain correction applied	eotvos
57	GED_Fourier_0	Enhanced Fourier derived Ged horizontal EW gravity gradient with no terrain correction applied	eotvos
58	GND_Fourier_0	Enhanced Fourier derived Gnd horizontal NS gravity gradient with no terrain correction applied	eotvos
59	GNE_Fourier_0	Enhanced Fourier derived Gne gravity curvature gradient with no terrain correction applied	eotvos
60	GUV_Fourier_0	Enhanced Fourier derived Guv gravity curvature gradient with no terrain correction applied	eotvos
61	DrapeSurface_Fourier	Drape surface for enhanced Fourier reconstruction (smoothed flight surface)	metres

Table 5: Final FALCON® AGG Digital Data – ASEG GDF-II (ASCII) format

File	Description	Units
DTM	Terrain (height above EGM96 geoid), 20 m grid cell, with DEM-S extension (Trimmed for easy display)	metres
DTM_full	Terrain (height above EGM96 geoid), 20 m grid cell, with DEM-S extension, for AGG processing	metres
Fourier_drape_surface	Drape surface for Fourier reconstruction (smoothed flight surface) height above EGM96 geoid	metres
Fourier_gD_0	Enhanced Fourier derived vertical gravity, no terrain correction applied	mGal
Fourier_gD_0_conformed	Enhanced Fourier derived vertical gravity, no terrain correction applied, conformed to regional gravity	mGal
Fourier_GDD_0	Enhanced Fourier derived vertical gravity gradient, no terrain correction applied	eotvos
Fourier_GDD_0_conformed	Enhanced Fourier derived vertical gravity gradient, no terrain correction applied, conformed to regional gravity	eotvos
Fourier_gD_2p1	Enhanced Fourier derived vertical gravity, terrain correction density 2.1 g/cm^3	mGal
Fourier_gD_2p1_conformed	Enhanced Fourier derived vertical gravity, terrain correction density 2.1 g/cm^3, conformed to regional gravity	mGal
Fourier_GDD_2p1	Enhanced Fourier derived vertical gravity gradient, terrain correction density 2.1 g/cm^3	eotvos
Fourier_GDD_2p1_conformed	Enhanced Fourier derived vertical gravity gradient, terrain correction density 2.1 g/cm^3, conformed to regional gravity	eotvos
Fourier_gD_2p67	Enhanced Fourier derived vertical gravity, terrain correction density 2.67 g/cm^3	mGal

Fourier_gD_2p67_conformed	Enhanced Fourier derived vertical gravity, terrain correction density 2.67 g/cm^3, conformed to regional gravity	mGal
Fourier_GDD_2p67	Enhanced Fourier derived vertical gravity gradient, terrain correction density 2.67 g/cm^3	eotvos
Fourier_GDD_2p67_conformed	Enhanced Fourier derived vertical gravity gradient, terrain correction density 2.67 g/cm^3, conformed to regional gravity	eotvos

Table 6: Final FALCON® AGG Grids – ERMapper format